Confidential Offer for Complete Acquisition

US Patent 12,650,086 B1

Device for Conversion of Kinetic and Thermal Energies of Gas Flows to Work

INDICATIVE CONSIDERATION
US$20,000,000

This document presents the Seller's proposed terms for the complete acquisition of the patent and associated technology package. It is intended to facilitate commercial evaluation, due diligence and negotiation. Except for any separately executed confidentiality obligations, it does not create a binding obligation on either party. A binding transaction will arise only upon execution of a definitive written patent assignment and asset sale agreement.

Discounted Price and Development-Stage Disclaimer

The proposed US$20 million consideration is a discounted strategic price that reflects the technology's current development stage and the risks assumed by the Purchaser.

The system is suitable only for gas streams meeting defined operating conditions.

The design is source-specific: turbine maps, nozzle performance, pressure losses, materials and control settings depend on the selected industrial source, and a generic prototype may produce results that are commercially irrelevant. For this reason, the reported performance is based on more generalised mathematical and engineering modelling.

The technical and financial figures are screening scenarios rather than guarantees or forecasts. The Purchaser will therefore bear the cost and risk of physical validation and site integration.

2026

1. The offer

The patent owner and seller (Seller) invites a suitably qualified purchaser (Purchaser) to acquire the complete patent and technology package associated with US Patent 12,650,086 B1. The proposed transaction is a complete and permanent assignment for a single payment of US$20,000,000. Following completion, no continuing licence fee, royalty or revenue-sharing payment would be payable to the Seller unless the parties separately agree to additional services.

> **Offer position:**
>
> US$20,000,000 payable once in cleared funds at completion for the agreed patent and technology assets. The offer is confidential, indicative and non-binding until definitive transaction documents are executed.

2. The patented system

The patented system is intended to convert kinetic, pressure and thermal energy carried by a moving gas stream into mechanical work or electricity. Annexure A reproduces the issued United States patent and its drawing, description and claims. The architecture places at least two turbines in sequence within a duct extending from a gas-flow inlet to an atmospheric outlet. A measurement section is located immediately before the primary generating turbine, while a controlled cooling and pressure-management section is located between that turbine and the downstream flow-control component. Pressure and temperature are measured before the primary turbine, within the cooling section and at the atmospheric outlet. A controller uses those measurements to regulate an evaporating-liquid injector positioned at or immediately after the primary turbine.

The gas first passes through the primary generating turbine, which extracts useful work. The injector then produces a controlled mist in the downstream cooling section. As the liquid evaporates, it absorbs latent heat and changes the gas temperature, density, composition and mass flow. The intended effect is to reduce pressure and temperature immediately downstream of the primary turbine, thereby increasing the useful pressure and temperature differential available across it. The controller adjusts the injection rate from measured operating conditions while maintaining the required pressure margin above the surrounding atmosphere. In the patent's general architecture, the downstream turbine may help restrict atmospheric-air intrusion and may recover residual flow energy. In the specific operating case used by the supplied simulator, the downstream component is used principally to regulate discharge and limit reverse atmospheric flow, and no electrical output is credited to it.

> **Operating sequence:**
>
> Known gas stream and ambient conditions -> primary generating turbine extracts work -> controlled liquid injection and evaporation in the downstream cooling section -> downstream component regulates discharge and limits atmospheric backflow -> release to atmosphere.

3. Mathematical and engineering model, development framework and simulator

The package includes a comprehensive mathematical and engineering development framework together with a self-contained browser-based System Performance and Design Optimisation Simulator. The model is not limited to the equations presently executed by the browser application. It translates the patented architecture into a structured basis for source qualification, system sizing, component selection, control development, software implementation, test planning and staged physical validation.

3.1 Engineering development framework

The model establishes a complete engineering variable and data inventory for the gas source, thermodynamic state, flow path, generating turbine, downstream flow-control component, liquid properties, atomisation and evaporation, pump, reservoir and piping, generator and electrical load, sensors, actuators, structural limits, materials and environmental constraints. This inventory provides an engineer with a defined list of measurements, manufacturer data, assumptions and design decisions required to progress from the patent description to a site-specific engineering study.

It separates fixed design variables from operating commands, physically solved state variables and uncertain inputs. Geometry, turbine and generator ratings, nozzle count and size, liquid-delivery equipment and reservoir capacity can therefore be selected in an outer design process, while injection rate, loading and other adjustable settings are optimised for each operating condition. Pressure, temperature, density, humidity, flow and rotor states are solved by the model rather than treated as arbitrary selections, and uncertain quantities can be tested through scenario envelopes or probability-based sampling.

The framework defines a staged model-fidelity pathway. A rapid screening model supports early source rejection and coarse design searches; an engineering model adds fuller conservation balances, psychrometrics, calculated losses, sizing and dynamic control; a calibrated model incorporates measured turbine maps, pump and valve curves, nozzle behaviour, evaporation calibration and measured auxiliary demand; and selected finalist designs can be transferred into computational fluid dynamics, structural analysis or external component co-simulation. This gives the purchaser a defined route for increasing confidence without requiring every candidate to be analysed initially at the highest cost and complexity.

The thermodynamic and flow treatment covers humid-gas properties, pressure-dependent saturation temperature and latent heat, conventional droplet evaporation, isenthalpic flash evaporation, high-temperature gas-driven evaporation, vapour addition, incomplete evaporation, liquid carryover, mixing and duct losses, turbine and generator performance, pump and auxiliary demand, net power, net energy and exergy. It distinguishes whether boiling is thermodynamically possible from whether a particular boiling heat-transfer regime has actually been established, and it exposes the active evaporation regime, limiting constraint and calculation status.

The model also supplies the engineering logic needed to size and specify the principal system elements. It provides methods and data requirements for the flow area and residence length, rotor and shaft operating limits, generator and load rating, injector-orifice area and nozzle count, droplet-size target, pump duty, reservoir volume, liquid-line sizing, pressure losses, instrumentation ranges and control limits. Pressure reserve, temperature, evaporation, carryover, Mach number, rotational speed, structural, electrical, pump, map-domain, property-domain and numerical-convergence requirements are treated as constraints rather than being concealed within a single output number.

Beyond steady performance, the framework addresses multiobjective and robust optimisation, sensitivity and uncertainty analysis, operating schedules, start-up and shutdown logic, pressure control, generator loading, fault handling, protective trips, independent overspeed and emergencyshutdown functions, programmable-controller implementation, instrumentation selection and hazardous-area considerations. It includes a commissioning and verification sequence covering sensor calibration, actuator tests, dynamic-response identification, failure scenarios, safe-state proof and measured confirmation of net electrical improvement.

The software and verification specification requires explicit unit handling, separation of absolute, gauge and differential pressure, structured feasibility and failure statuses, conservation residuals, limiting-case tests, regression tests, optimiser tests, calibration records, reproducible seeds, versioned inputs, persistent logs, checkpoints, machine-readable outputs and a human-readable recommendation report. These provisions make the work transferable and auditable and provide a basis for another engineering team to reproduce, challenge, calibrate and extend the analysis.

3.2 Purpose of the simulator

The browser simulator is the current screening-level implementation of the wider engineering framework. It is intended to assist engineers who know, or can measure, the input conditions of a potential gas source. The principal inputs are inlet gas velocity, absolute pressure, temperature and relative humidity; ambient pressure, temperature and humidity; operating duration; available manufacturer performance data or capacity assumptions; pressure-loss and reverse-flow assumptions; pump and auxiliary characteristics; and permissible operating limits.

For those known inputs, the simulator searches the permitted design and operating space to identify feasible and comparatively optimal values for the common flow area, the length of the cooling and evaporation section, the target droplet size, the liquid-to-dry-gas ratio, the injection flow rate and any physically adjustable downstream control setting. It calculates the pressure and temperature after the primary turbine, the available differential and turbine output, evaporation and carryover, pump and auxiliary demand, net power and energy, active constraints and the difference between dry and injection-assisted operation. It also records calculation status, sensitivity, uncertainty, logs, tables and exportable figures.

The zero-injection case is evaluated using the same physical design and boundary conditions. The simulator should select zero injection whenever liquid addition does not improve net exported electricity after pump, downstream flow-control and other auxiliary demands. Its outputs are bounded design-development recommendations and a means of identifying infeasible combinations and missing data.

3.3 Engineering transfer and development value

The purchaser would therefore receive more than a patent document and an executable calculator. The package contains an organised engineering development roadmap that can be used to screen candidate sites, define measurement campaigns, prepare requests for turbine, pump, injector, generator and instrumentation data, compare design alternatives, identify active constraints, plan prototype tests, calibrate the model and prepare controlled operating schedules. It also provides a common technical language for thermodynamic, mechanical, electrical, controls, safety and software specialists working on the same development programme.

This body of work can reduce the time, cost and uncertainty involved in converting the patent into a purchaser-led research, prototype and commercialisation programme. It provides a documented foundation for integrating measured component maps, commissioning data, computational fluid dynamics and structural analysis, and for evaluating future improvements or derivative configurations. That development value supports the completeness of the transferred package and the strategic asking price, while remaining subject to the technical-validation qualifications stated in this offer.

4. Package assets and Annexures

The acquisition includes the Seller's assignable interest in the United States patent; the comprehensive mathematical and engineering model; the technical analysis and model specification; the browser simulator and source code; the variable inventory and data requirements; thermodynamic, flow, sizing and component-selection methods; control, instrumentation, safety and commissioning architecture; verification, calibration and acceptance plans; datasets; focused and broad screening results; calculation outputs; documented know-how; and assignable copyright. Related patent rights are included only where owned by the Seller and expressly scheduled in the definitive agreement.

Annexure A:

Annexure A is the copy of US Patent 12,650,086 B1. It provides the formal patent drawing, system description and claims defining the protected architecture, including the inlet and outlet duct, the primary and downstream turbines, the measurement sections before and between the turbines, the liquid injector, sensors and controller.

Annexure B:

Annexure B is the evidence review of global waste heat. It identifies an indicative gross global waste-heat order of magnitude near 320 EJ per year, published economic recovery estimates equivalent to approximately 6–9% of global energy input, and an estimated 69.1 EJ of waste-heat exergy. That exergy estimate includes approximately 14.4 EJ between 100°C and 300°C and 24.1 EJ above 300°C.

For patent-specific commercial screening, Annexure B identifies the 14.4 EJ medium-temperature category as the closest published global proxy for the simulator's favourable inlet-temperature range. Applying an indicative compatibility screen of 10–25% produces a preliminary patent-relevant candidate pool of approximately 1.44–3.60 EJ per year, equivalent to about 400–1,000 TWh per year of exergy. This is a source-screening range and not a forecast of electricity generation, revenue or technically recoverable output.

Annexure C: comparative-energy findings. Annexure C presents the evaluated downstream flow-control operating case, tested input ranges, figures and engineering recommendations. Its best-found point occurs at 419 K, 142.2 kPa(a), 45 m/s and 0% relative humidity, with a common 2.0 m² flow area through the inlet and cooling section, an 8.0 m cooling and evaporation length, a 20 µm target droplet diameter and a liquid-to-dry-gas ratio of 0.03926 kg/kg. The reported net power increases from 1.1441 MW dry to 1.3646 MW with injection, an increase of 220.5 kW or 19.27%, equivalent to 1.764 MWh over eight hours. Representative screenshots of the simulator input interface, reproduced calculation results and embedded mathematical-model documentation are included in Appendix C1 of Annexure C. A controlled live demonstration of the executable simulator may be provided to a suitably qualified prospective purchaser following execution of an appropriate confidentiality agreement.

5. Financial opportunity

The closest available global proxy for the patented system is Annexure B's estimate of 14.4 EJ per year of waste-heat exergy between 100°C and 300°C. The available evidence does not identify how much of that resource also satisfies the required gas form, pressure, velocity, humidity, operating continuity and installation conditions. The financial calculation therefore applies an indicative compatibility range of 10–25%.

The calculation assumes that a conventional dry recovery system converts 30% of the compatible exergy into electricity and then applies the injection-assisted simulator uplift to that electricity output. The uplift is not applied directly to gross waste heat.

At the focused-screen median increase of 13.18%, the indicated additional electricity is approximately 15.8–39.5 TWh per year, with a gross annual electricity value of approximately US$1.58–3.95 billion at US$0.10/kWh.

At the focused-screen mean increase of 13.30%, the indicated additional electricity is approximately 16.0–39.9 TWh per year, with a gross annual value of approximately US$1.60–3.99 billion.

At the best-found increase of 19.27%, the technical upside screen indicates approximately 23.1–57.8 TWh per year of additional electricity, with a gross annual value of approximately US$2.31–5.78 billion.

These values are global screening scenarios rather than forecasts. They exclude capital expenditure, operating costs, downtime, water supply, site integration, transmission losses, commercial sharing, financing, taxation and technical-development risk.

> **Selected 25% compatibility case:**
>
> Approximately 39.5 TWh of additional electricity and US$3.95 billion of gross annual electricity value using the focused-range median increase.

6. Valuation and proposed consideration

Using the selected 25% compatibility case and the focused-range median result, the indicated global gross electricity benefit is approximately US$3.95 billion per year. An illustrative strategic-purchaser case assumes eventual participation in 3% of that opportunity, corresponding to approximately US$118.6 million per year of gross electricity value associated with the Purchaser's projects.

If 25% of that project value is retained after operating costs and commercial sharing, the mature annual economic benefit is approximately US$29.7 million. Applying the delayed commercialisation factor used in the valuation analysis gives approximately US$46.6 million before technical and commercial probability weighting and approximately US$9.3 million after applying a 20% success weighting.

The focused-range mean case produces a similar probability-weighted value of approximately US$9.4 million, while the best-point upper case produces approximately US$13.6 million.

These probability-weighted calculations do not include the strategic value of complete control, freedom from continuing royalties, defensive value, simulator and source-code ownership, documented know-how, development time already invested, selected-site upside, future improvements or derivative patent filings.

The comprehensive mathematical and engineering model has additional development value that is not captured by the electricity-income calculation. A purchaser beginning with the patent alone would still need to define the full variable set, property methods, conservation structure, design and operating-variable separation, sizing rules, control philosophy, software architecture, uncertainty treatment, verification tests, instrumentation requirements and commissioning pathway. The supplied package substantially advances that work and gives the purchaser a structured basis for engaging specialist engineers, component manufacturers, test facilities and commercial partners.

Indicative purchase price:

The proposed one-off acquisition price is US$20,000,000. This price is a strategic transaction position rather than the output of the probability-weighted income calculation alone. It reflects complete ownership of the patent and associated technical package, the absence of continuing royalties, transfer of the simulator and source code, and transfer of a substantial engineering development framework covering source qualification, thermodynamics, sizing, component and instrumentation selection, optimisation, control, safety, software implementation, verification and commissioning. It also reflects the Purchaser's control of future technical improvements, derivative configurations and commercial upside.

7. Territorial and technical scope

Outside protected territories, commercial value may arise from simulator copyright, confidential know-how, development lead time, contractual protection and future patent filings.

8. Indicative commercial terms

The proposed consideration is US$20,000,000, payable once in cleared United States dollars at completion. The transaction is intended to be a permanent assignment of the patent, software, mathematical model, technical documents, scheduled data and know-how assets included in the definitive agreement. No continuing licence fee, royalty or revenue-sharing payment is proposed after completion.

9. Due diligence and completion

The Purchaser should independently verify patent ownership and status, maintenance records, source-code and copyright provenance, third-party rights, technical assumptions, model outputs, market evidence and financial projections. The definitive agreement should identify transferred and excluded assets and address payment, assignment, confidentiality, limited representations, liability, taxes, recordation, pending rights and handover. At completion, executed patent and copyright assignments, the simulator and source-code package, technical documents, scheduled data and defined know-how handover should be delivered against release of the full purchase price.

10. Next step and non-binding status

A Purchaser wishing to proceed should provide a written expression of interest identifying its legal entity, authorised contact, financial capacity, requested due-diligence period and proposed conditions to:

Benedict de St. Amatus, PhD (Adelaide), Dipl.-Ing. (St. Petersburg), GradDip IP (UTS), D.N.Lit.

Solarius Technologies Pty Ltd (ABN: 83 667 177 353)

Queensland, Australia

Tel: +61 (4) 1028 9237

E-mail: b.stamatus@ausihem.org

The Seller may accept, reject, withdraw or amend this offer before a definitive agreement is executed. No prior communication creates a binding transfer.

ANNEXURE A

US Patent 12,650,086 B1

Device for Conversion of Kinetic and Thermal Energies of Gas Flows to Work

2026

US012650086B1

(12) **United States Patent**
de St. Amatus et al.

(10) **Patent No.: US 12,650,086 B1**
(45) **Date of Patent: Jun. 9, 2026**

(54) **DEVICE FOR CONVERSION OF KINETIC AND THERMAL ENERGIES OF GAS FLOWS TO WORK**

(71) Applicants: **Benedict de St. Amatus**, Forest Glen (AU); **Alexander de St. Amatus**, Forest Glen (AU)

(72) Inventors: **Benedict de St. Amatus**, Forest Glen (AU); **Alexander de St. Amatus**, Forest Glen (AU)

(*) Notice: Subject to any disclaimer, the term of this patent is extended or adjusted under 35 U.S.C. 154(b) by 0 days.

(21) Appl. No.: **19/195,430**

(22) Filed: **Apr. 30, 2025**

(51) **Int. Cl.**
F03D 1/02 (2006.01)
F01D 21/00 (2006.01)
F01D 25/30 (2006.01)

(52) **U.S. Cl.**
CPC ***F01D 25/305*** (2013.01); ***F01D 21/003*** (2013.01); *F05D 2260/212* (2013.01); *F05D 2270/301* (2013.01); *F05D 2270/303* (2013.01)

(58) **Field of Classification Search**
CPC ... F03D 1/02; F03D 1/025; F03D 1/04; F03D 1/041; F03D 1/042; F03D 1/044; F03D 1/051; F03D 1/053; F03D 7/00; F03D 9/00; F03D 9/007; F03D 9/008; F03D 9/14; F03D 9/18; F03D 9/28; F03D 9/35; F03D 9/37; F03D 9/39; F03D 80/60; F03D 80/601; F03D 9/41; F03D 17/018; F03D 17/009; F03D 17/022; F03D 17/026; F01D 25/305; F01D 21/003; F05D 2260/212; F05D 2270/301; F05D 2270/3011; F05D 2270/3013; F05D 2270/3015; F05D 2270/303
See application file for complete search history.

(56) **References Cited**

U.S. PATENT DOCUMENTS

4,801,811 A * 1/1989 Assaf F03D 9/25 290/55
4,878,349 A * 11/1989 Czaja F03G 7/04 60/641.14
5,174,724 A * 12/1992 Ammons F03D 3/062 290/55

(Continued)

FOREIGN PATENT DOCUMENTS

WO WO-2007118282 A1 * 10/2007 .... F22B 1/1853

OTHER PUBLICATIONS

Volker, Dietz, "Power Plant or Energy Transducer . . . " EPO, DE 102012017707A1 Mar. 13, 2014 (Year: 2014).*

Primary Examiner — Nathaniel E Wiehe
Assistant Examiner — Joshua R Beebe

(57) **ABSTRACT**

An energy conversion device transforms kinetic and thermal energies of gas flows into usable work. It features a duct with an inlet and outlet for the gas flow and a cascade of at least two turbines located in distinct zones of the duct. A post-turbine gas cooling system, associated with the first turbine, includes an injector of evaporating liquid regulated by a controller using real-time data from pressure and temperature gauges. The first turbine's performance is enhanced by pressure and temperature differentials created by the cooling system. The second turbine prevents ambient air intrusion and further converts residual kinetic energy. Both turbines can be coupled either to electric generators or to mechanical devices or both for converting the turbines work output either to electricity or to mechanical work or to both.

3 Claims, 1 Drawing Sheet

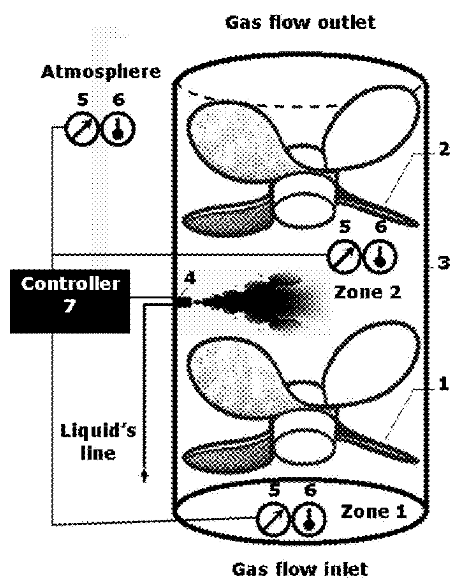

(56) **References Cited**

U.S. PATENT DOCUMENTS

7,821,151	B2 *	10/2010	Le	F03G 6/045 290/43
8,727,698	B1 *	5/2014	Pickett	F03D 9/25 415/909
2013/0285378	A1 *	10/2013	Carmein	F03D 7/00 290/44

* cited by examiner

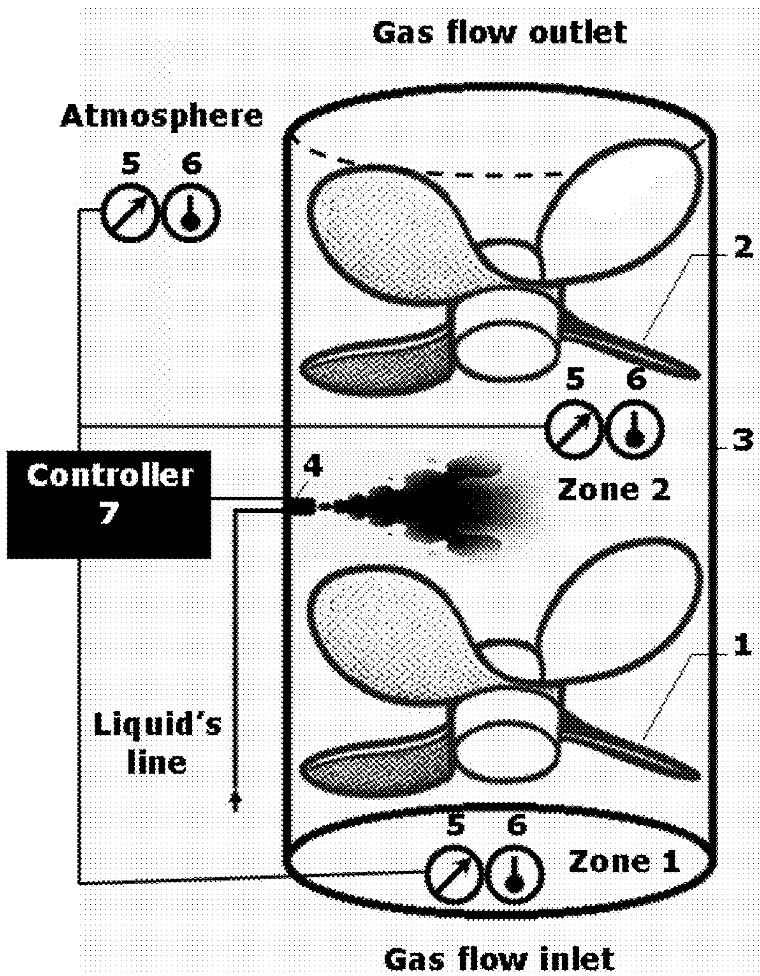
Gas flow outlet
Atmosphere
5
6
2
5
6
3
Controller
7
4
Zone 2
1
Liquid's
line
5
6
Zone 1
Gas flow inlet

DEVICE FOR CONVERSION OF KINETIC AND THERMAL ENERGIES OF GAS FLOWS TO WORK

CROSS-REFERENCE TO RELATED APPLICATIONS

Not Applicable

STATEMENT REGARDING FEDERALLY SPONSORED RESEARCH OR DEVELOPMENT

Not Applicable

REFERENCE TO SEQUENCE LISTING, A TABLE, OR A COMPUTER PROGRAM LISTING COMPACT DISC APPENDIX

Not Applicable

FIELD OF THE INVENTION

The present invention relates generally to energy conversion systems. More specifically, it pertains to the field of systems for conversion of kinetic and thermal energies of gases into usable work. The invention has applications in renewable power generation, waste heat utilisation, and other areas where the conversion of kinetic and thermal energies of gases into mechanical or electrical work, or both, is desired.

DESCRIPTION OF RELATED ART

The reference in this specification to any prior publication (or information derived from it), or to any matter which is known, is not, and should not be taken as an acknowledgment or admission or any form of suggestion, that the prior publication (or information derived from it) or known matter forms part of the common general knowledge in the field of endeavour, to which this specification relates.

Traditional energy conversion systems often involve the use of turbines to convert the kinetic energy of gases into mechanical work. These systems typically include a turbine through which gas is passed and energy is extracted. For example, wind turbines are widely used to convert the kinetic energy of wind into electrical energy. They consist of rotor blades that capture the wind's kinetic energy, which is then converted into mechanical energy to drive a generator.

One significant disadvantage of wind turbines is their inability to capture the thermal energy of the gas flow, which leads to a substantial amount of wasted energy. This limitation reduces the overall efficiency of the system and increases operational costs due to the underutilisation of available energy resources. Given this limitation, there is a need for an improved energy conversion system that maximises the extraction of usable work from both the kinetic and thermal energies of gases.

OBJECT OF THE INVENTION

The object of the present invention is to provide a device for conversion of kinetic and thermal energies of gases to work that overcomes the drawbacks of the prior art. Specifically, the invention aims to:

Maximise the extraction of usable work from both the kinetic and thermal energies of the gases.

Provide control over the energy conversion process through real-time monitoring and adjustment of operational parameters.

Offer a versatile solution that can be adapted to various industrial, waste heat management, and renewable power generation applications.

Reduce operational costs and environmental impact by improving the overall efficiency of the energy conversion process.

Other objects and advantages of the present invention will become apparent from the following description, taken in connection with the accompanying drawings, wherein, by way of illustration and example, embodiments of the present invention are disclosed.

SUMMARY OF THE INVENTION

According to the present invention, the device for the conversion of kinetic and thermal energies of gases to work, comprises a duct having an inlet for gas flow entry and an outlet for gas flow exit to the ambient atmosphere; a cascade of at least a first turbine and a second turbine positioned within the duct, wherein the first turbine is positioned in a first zone located between the duct inlet and said first turbine, and the second turbine is positioned in a second zone located between the first turbine and the duct outlet; a post-turbine gas cooling system associated with the first turbine, comprising at least one injector of evaporating liquid positioned at or near the outlet of the first turbine, and at least three pressure gauges and at least three temperature gauges distributed in the first zone, the second zone, and outside the duct, and a controller for controlling the injector based on the pressure and temperature data from the gauges.

At least one pressure gauge and at least one temperature gauge are positioned in each of the first and second zones for measuring respective pressures and temperatures and transferring real-time data to the controller. At least one pressure gauge and at least one temperature gauge are positioned outside the duct for measuring the ambient atmospheric pressure and temperature and transferring real-time data to the controller.

The injector is connected to a liquid's line comprising pipes, at least one reservoir for the liquid, at least one filter and at least one pump. The injector injects a mist of evaporating liquid into the gas flow post the first turbine, inducing rapid cooling and a consequent pressure drop at or near the outlet of the first turbine, wherein the controller uses an algorithm configured to regulate the injection rate of the evaporating liquid based on the real-time pressure and temperature data to maintain preferred pressure and temperature differentials between the first and second zones, and between the second zone and the ambient atmosphere.

The first turbine converts a fraction of the kinetic energy of the gas flow entering the duct into work, with its conversion rate enhanced by the pressure and temperature differentials created by the gas flow's cooling system between the turbine's inlet and outlet. The second turbine is used to prevent ambient air intrusion into the second zone and to further convert a fraction of the residual kinetic energy of the gas flow in the second zone to work. The work produced by the device is the cumulative work of the first and second turbines.

The first and the second turbines are coupled either to electric generators or to mechanical devices or both for converting the turbines work output either to electricity or to mechanical work or to both.

BRIEF DESCRIPTION OF THE DRAWING

By way of illustration only, an embodiment of the invention is described more fully hereinafter with reference to the accompanying drawing, in which FIG. **1** shows an embodiment of a device for the conversion of kinetic and thermal energies of gases to work.

DETAILED DESCRIPTION OF THE INVENTION

The embodiment of the device for the conversion of kinetic and thermal energies of gases to work is shown with references to FIG. **1**.

FIG. **1** shows the device for the conversion of kinetic and thermal energies of gases to work, wherein said device comprises at least one cascade of turbines. Said cascade comprises at least of two turbines-Turbine **1** and Turbine **2**, which are positioned inside a Duct **3**. Duct **3** has an inlet for gas flow entry and an outlet for gas flow exit to the ambient atmosphere. Duct **3** is zoned in at least two zones: Zone **1**, which is located between the inlet of Duct **3** and Turbine **1** and Zone **2**, which is located between Turbine **1** and Turbine **2**. Turbine **2** is located at or near the outlet of Duct **3**.

Alternative embodiments of said device may comprise multiple cascades of turbines and more than two turbines in a cascade.

Turbine **1** converts a fraction of the gas flow's kinetic energy into work, with its performance enhanced by the pressure and temperature differentials between Zones **1** and **2** created by a post-turbine gas cooling system. Turbine **2** is used to prevent ambient air intrusion into Zone **2** and to further convert a fraction of the residual kinetic energy of the gas flow in said zone to work.

The work produced by the device is the cumulative work of Turbines **1** and **2**.

Said post-turbine gas cooling system comprises at least one Injector **4** of an evaporating liquid into the gas flow, at least three Pressure Gauges **5**, at least three Temperature Gauges **6**, and a mechanical or a digital Controller **7** that controls the Injector **4**.

Injector **4** is positioned at or near the outlet of Turbine **1** (the pipes and the reservoir and the filter and the pump of the liquid's line are not shown in the FIGURE).

At least one Pressure Gauge **5** and at least one Temperature Gauge **6** are located in Zone **1**, measuring the pressure and the temperature in said zone and transferring the real-time data to the Controller **7**.

At least one Pressure Gauge **5** and at least one Temperature Gauge **6** are located in Zone **2**, measuring the pressure and the temperature in said zone and transferring the real-time data to the Controller **7**.

At least one Pressure Gauge **5** and at least one Temperature Gauge **6** are located outside the Duct **3**, measuring the pressure and the temperature of the ambient atmosphere and transferring the real-time data to the Controller **7**.

Injector(s) **4** inject(s) mist of evaporating liquid into the gas flow. The mist of evaporating liquid mixes with the gas flow and evaporates. The evaporation of the liquid rapidly cools the gas flow, which creates a pressure drop at or near the outlet of Turbine **1**. The pressure difference that is created between Zones **1** and **2** of the Duct **3** results into a partial utilisation of the thermal energy of the gas flow to work.

Controller **7** receives pressure and temperature real-time data from the Pressure Gauges **5** and the Temperature Gauges **6** for Zones **1** and **2** of the Duct **3**, and for the ambient atmosphere. Controller **7** uses an algorithm to optimise the injection rate of the evaporating liquid based on real-time pressure and temperature data. Based on this data, Controller **7** commands Injector(s) **4** to inject an amount of the evaporating liquid at a rate that is sufficient to create pressure and temperature drops between Zones **1** and **2**, and between Zone **2** and the ambient atmosphere, wherein the pressure and the temperature of the gas flow in Zone **1** is the higher than the pressure and the temperature of the gas flow in Zone **2**, and the pressure and the temperature of the gas flow in Zone **2** is higher than the pressure and the temperature of the ambient atmosphere.

Turbines **1** and **2** are coupled either to electric generators or to mechanical devices or both for converting the turbines work output either to electricity or to mechanical work or to both.

The invention claimed is:

1. A device for conversion of kinetic and thermal energies of gas flows to work, comprising:

(a) a duct having an inlet for gas flow entry and an outlet for gas flow exit to ambient atmosphere;

(b) a first turbine positioned within the duct such that a first zone is located between the duct inlet and the first turbine;

(c) a second turbine positioned within the duct such that a second zone is located between the first turbine and the second turbine, the second turbine being arranged downstream of the first turbine and upstream of the duct outlet;

(d) at least one injector positioned in the second zone downstream of the first turbine and upstream of the second turbine, the injector being configured to inject a mist of evaporating liquid into the gas flow after the gas flow has passed through the first turbine;

(e) a liquid line connected to the injector and comprising pipes, at least one reservoir for the liquid, at least one filter, and at least one pump;

(f) a first pair of gauges positioned in the first zone, the first pair comprising a pressure gauge and a temperature gauge for measuring local pressure and temperature in the first zone;

(g) a second pair of gauges positioned in the second zone, the second pair comprising a pressure gauge and a temperature gauge for measuring local pressure and temperature in the second zone;

(h) a third pair of gauges positioned outside the duct, the third pair comprising a pressure gauge and a temperature gauge for measuring ambient atmospheric pressure and temperature; and

(i) a controller configured to receive real-time pressure and temperature data from the first pair, the second pair, and the third pair and to regulate an injection rate of the evaporating liquid through the injector based on said real-time pressure and temperature data;

wherein the injector injects a mist of evaporating liquid into the gas flow in the second zone after passage through the first turbine, evaporation of the liquid rapidly cooling the gas flow and causing a pressure drop from the first zone to the second zone at or near an outlet side of the first turbine, and the controller maintaining pressure and temperature in the second zone above ambient atmospheric pressure and temperature.

2. The device of claim **1**, wherein the second turbine is positioned at or near the duct outlet and is configured to oppose ingress of ambient air from the duct outlet into the second zone and to convert a fraction of residual kinetic energy of the gas flow into work.

3. The device of claim **1**, wherein the controller uses an algorithm configured to command the injector to inject the evaporating liquid at a rate sufficient to maintain the pressure and temperature relationships between the first zone, the second zone, and the ambient atmosphere.

* * * * *

ANNEXURE B

US Patent 12,650,086 B1

Device for Conversion of Kinetic and Thermal Energies of Gas Flows to Work

A Comparative Evidence Review of Quantities, Major Contributors and Recovery Prospects of the Global Waste Heat

by Dr Benedict de St. Amatus

Solarius Technologies Pty Ltd (ABN: 83 667 177 353)

Queensland, Australia

2026

Executive summary

Waste heat is one of the largest underused energy streams in the world, but there is no single authoritative global inventory. Published estimates differ because they measure different things: total rejected energy, heat physically released to the environment, industrial heat above a chosen reference temperature, heat technically recoverable, or exergy capable of producing useful work. This report therefore separates gross waste heat, technical recovery potential, economic recovery potential and exergy rather than combining them into one misleading number.

Global energy demand in 2025 was approximately 620 EJ. The International Energy Agency (IEA) reported that demand increased by about 8 EJ, or 1.3%, during the year.[1] Applying the widely cited whole-energy-system estimate that waste heat is about 52% of input energy gives an indicative contemporary gross waste-heat order of magnitude of about 320 EJ per year.[2] This is a derived screening estimate, not an official inventory. A separate global scenario study found waste-heat emissions equal to 23–53% of input energy, with theoretical recovery equivalent to 6–12% and economic recovery equivalent to 6–9% of input energy.[3] An exergy-based study estimated 69.1 EJ of global waste-heat exergy, comprising 30.5 EJ below 100°C, 14.4 EJ between 100°C and 300°C, and 24.1 EJ above 300°C.[4]

The contemporary regional picture is highly uneven:

- China has the largest recent national inventory. A 2026 study estimated approximately 50 EJ of waste heat in 2021, of which 40.6 EJ, or 81%, was below 50°C.[5] An earlier whole-system study found waste heat equal to 42% of primary energy input in 2018; electricity generation supplied 45% of the total and industry held the highest-quality, mostly above-300°C resource.[6]
- The United States recorded 61.57 quadrillion Btu of rejected energy in 2023, equivalent to about 65 EJ, in the Lawrence Livermore National Laboratory national energy-flow accounting. This broad total includes conversion and end-use losses and is not identical to recoverable heat.[7] United States Department of Energy guidance estimates that 20–50% of industrial energy input is lost as waste heat.[8]
- EU-27 plus the United Kingdom has at least 960 PJ/year (267 TWh/year) of process-specific industrial flue-gas excess heat if exhaust gases are cooled to 25°C. About 230 PJ/year was spatially available to present district-heating areas, increasing in the study's future low-temperature-network cases to 258–679 PJ/year depending on the delivery temperature.[9]

---

[1] International Energy Agency (IEA) (2026) *Global Energy Review 2026*. Paris: IEA. Available at: https://www.iea.org/reports/global-energy-review-2026 (Accessed: 11 July 2026).
[2] Forman, C., Muritala, I.K., Pardemann, R. and Meyer, B. (2016) 'Estimating the global waste heat potential', *Renewable and Sustainable Energy Reviews*, 57, pp. 1568–1579. doi:10.1016/j.rser.2015.12.192.
[3] Firth, A., Zhang, B. and Yang, A. (2019) 'Quantification of global waste heat and its environmental effects', *Applied Energy*, 235, pp. 1314–1334. doi:10.1016/j.apenergy.2018.10.102.
[4] Bohra, A. and Vitta, S. (2022) 'Sustainability of large scale waste heat harvesting using thermoelectric', arXiv:2208.00616. Available at: https://arxiv.org/abs/2208.00616 (Accessed: 11 July 2026).
[5] Liu, Z., Yang, X., Sun, D. and Xia, J. (2026) 'Assessment of waste heat in China: Characteristics and national potential', *Energy*, 344, 139860. doi:10.1016/j.energy.2025.139860.
[6] Lin, Y., Chong, C.H., Ma, L., Li, Z. and Ni, W. (2022) 'Quantification of waste heat potential in China: A top-down Societal Waste Heat Accounting Model', *Energy*, 261, 125194. doi:10.1016/j.energy.2022.125194.
[7] Lawrence Livermore National Laboratory (LLNL) (2026) *Estimated U.S. Energy Consumption in 2023: 93.7 Quads*. Livermore, CA: LLNL. Available at: https://flowcharts.llnl.gov/commodities/energy (Accessed: 11 July 2026).
[8] U.S. Department of Energy (2026) 'Waste Heat Recovery Basics'. Washington, DC: DOE. Available at: https://www.energy.gov/cmei/ito/waste-heat-recovery-basics (Accessed: 11 July 2026).
[9] Manz, P., Kermeli, K., Persson, U., Neuwirth, M., Fleiter, T. and Crijns-Graus, W. (2021) 'Decarbonizing district heating in EU-27 + UK: How much excess heat is available from industrial sites?', *Sustainability*, 13(3), 1439. doi:10.3390/su13031439.

- India has no current whole-economy inventory of comparable quality. The best sectoral studies identify iron and steel, chemicals and petrochemicals, cement, pulp and paper, and glass as the principal industrial sources. One national sector study estimated that iron and steel alone offered up to 66.5 TWh of waste-heat-to-power potential under its modelling assumptions.[10]
- Middle East and North Africa (MENA) waste heat is concentrated in gas- and oil-fired power, refining and petrochemicals, LNG and gas processing, thermal desalination and oilfield flaring. Natural gas supplied 70% of regional electricity in 2024, while oil remained important in Iraq, Saudi Arabia and Kuwait.[11] Flaring is a distinct form of wasted chemical energy that ultimately becomes heat: global flaring reached 167 bcm in 2025, and Iran, Iraq, Libya and Algeria were among the nine countries responsible for more than four-fifths of the total.[12]
- Latin America, Sub-Saharan Africa and Oceania have significant site-level resources but poor national inventories. Their principal clusters are refining, oil and gas production, mining and mineral processing, steel, cement, aluminium/alumina, pulp and paper, food processing, thermal power and, increasingly, data centres.

The future will not be a simple increase or decrease. Waste heat from conventional thermal power and internal-combustion transport should decline in strong electrification and renewable-energy pathways. In contrast, low-grade heat from data centres, air conditioning, electrolysers, batteries, electric furnaces, industrial heat pumps, wastewater and urban infrastructure will rise. Global data-centre electricity use is projected to increase from about 415 TWh in 2024 to 945 TWh in 2030, creating a corresponding increase in concentrated low-temperature heat rejection.[13] Air-conditioning energy demand could triple by 2050 as the global stock approaches 5.6 billion units.[14]

Patent-relevant market screening: The associated system simulation identifies its strongest comparative performance in warm, dry gas streams, with a broad favourable inlet region of approximately 350–430 K (77–157°C), low relative humidity, absolute pressure around 120–180 kPa and available gas velocity around 25–45 m/s. The best-found point occurred at 419 K (145.9°C), 142.2 kPa absolute pressure, 45 m/s and 0% relative humidity. Within the separately examined focused optimal-input region, the modelled mean and median increases in net electrical output were above 12%, while the maximum reported comparative increase was 19.27%.

Existing international waste-heat inventories do not jointly classify temperature, pressure, velocity, humidity and operating continuity, so the exact global quantity suitable for the patented system cannot be directly measured. The closest quantified global proxy is the estimated 14.4 EJ/year of waste-heat exergy between 100°C and 300°C. Applying an indicative 10–25% compatibility screen for temperature, gas form, dryness, pressure, velocity, duty cycle and practical deployment gives a patent-relevant candidate pool of approximately 1.44–3.60 EJ/year, equivalent to about 400–1,000 TWh/year. This is a commercial screening range rather than a forecast of recoverable electricity and must be reduced further for conversion efficiency, site integration, capital cost and physical validation.

---

[10] Saha, B.K., Chakraborty, B. and Dutta, R. (2020) 'Estimation of waste heat and its recovery potential from energy-intensive industries', *Clean Technologies and Environmental Policy*, 22, pp. 1795–1814. doi:10.1007/s10098-020-01919-7.

[11] International Energy Agency (IEA) (2025) *The Future of Electricity in the Middle East and North Africa*. Paris: IEA. Available at: https://www.iea.org/reports/the-future-of-electricity-in-the-middle-east-and-north-africa (Accessed: 11 July 2026).

[12] World Bank (2026) *Global Gas Flaring Tracker Report 2026*. Washington, DC: World Bank. Available at: https://www.worldbank.org/en/programs/gasflaringreduction/publication/2026-global-gas-flaring-tracker-report (Accessed: 11 July 2026).

[13] International Energy Agency (IEA) (2025) *Energy and AI*. Paris: IEA. Available at: https://www.iea.org/reports/energy-and-ai (Accessed: 11 July 2026).

[14] International Energy Agency (IEA) (2018) *The Future of Cooling*. Paris: IEA. Available at: https://www.iea.org/reports/the-future-of-cooling (Accessed: 11 July 2026).

1. Scope, definitions and evidence method

1.1 What is counted as waste heat

Waste heat is thermal energy discharged from an energy conversion or production process because it is not used within the process boundary. It may leave as flue gas, cooling water, warm air, wastewater, hot products or solids, radiation, conduction, condenser heat, engine exhaust or cooling-tower discharge.

For policy and investment purposes, four levels must be distinguished:

1. Gross or theoretical heat: all thermal energy above a selected environmental reference state.
1. Technical potential: the portion accessible with feasible heat exchangers, heat pumps, power cycles, storage or networks after process constraints.
2. Economic potential: the portion competitive after capital cost, operating hours, distance, temperature lift and alternative-energy prices.
3. Exergy: the maximum useful work theoretically obtainable as the stream approaches environmental equilibrium.

The European Commission Joint Research Centre advises that heat should be treated as waste only when it is a by-product, cannot reasonably be avoided or recovered within the originating process, and is genuinely available for external use.[15] This prevents efficient cogeneration heat or deliberately produced steam from being counted as free waste heat.

1.2 Why published quantities differ

National studies use different reference temperatures, boundaries and recovery assumptions. Cooling a flue gas to 25°C produces a much larger theoretical number than cooling it to 100°C to avoid condensation or corrosion. A national Sankey diagram includes transport and power-generation losses, while an industrial survey may include only stack gas from selected sectors. Some studies report energy, others exergy, and some report potential electricity rather than heat.

The international review by Miró, Brückner and Cabeza collected industrial waste-heat estimates for 33 countries but found major comparability problems and identified substantial information gaps in Asia, South America, Africa and Oceania.[16] The same limitation remains evident in 2026. Accordingly, regional numbers in this report are labelled by boundary and confidence rather than added into a false global total.

1.3 Unit conversions

Unit	Equivalent
1 EJ	277.78 TWh
1 TWh	3.6 PJ
1 quadrillion Btu (quad)	1.055 EJ
1 Mtoe	0.04187 EJ
1 bcm natural gas	approximately 0.035–0.040 EJ lower heating value, depending on composition

[15] Lyons, L., Kavvadias, K. and Carlsson, J. (2021) *Defining and accounting for waste heat and cold*. EUR 30869 EN. Luxembourg: Publications Office of the European Union. doi:10.2760/73253.
[16] Miró, L., Brückner, S. and Cabeza, L.F. (2015) 'Mapping and discussing industrial waste heat potentials for different countries', *Renewable and Sustainable Energy Reviews*, 51, pp. 847–855. doi:10.1016/j.rser.2015.06.035.

2. Contemporary global magnitude and source structure

2.1 Gross energy-loss perspective

The IEA's 2025 global demand estimate implies an energy system using roughly 620 EJ annually.[17] Forman et al. estimated that 72% of primary energy was lost after conversion and that waste heat itself represented approximately 52% of global input energy.[18] On a contemporary 2025 base, this suggests about 324 EJ/year of gross heat discharge. The estimate is useful for scale but should not be interpreted as a recoverable resource: much of it is diffuse, close to ambient temperature or remote from a heat sink.

Firth, Zhang and Yang modelled power generation, industry, transport and buildings across several 2030 energy scenarios. Their total waste-heat result ranged from 23% to 53% of energy input. Theoretical recovery was 6–12% and economic recovery 6–9% of global input energy.[19] The large gap between emitted and economic potential reflects temperature quality, intermittency, transport distance and capital cost.

Figure 1 compares the energy-system quantities discussed above while retaining their different definitions and boundaries.

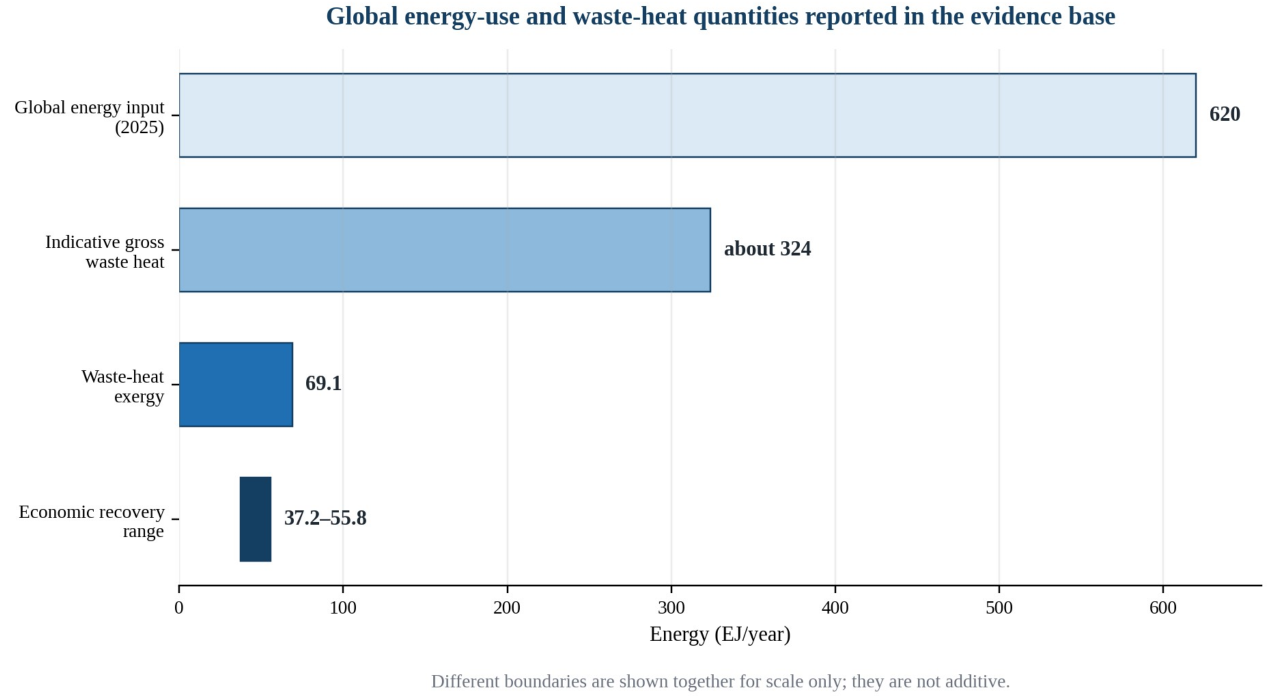

Figure 1. Global energy input, indicative gross waste heat, estimated waste-heat exergy and economic recovery range. The quantities use different system boundaries and are not additive.

[17] International Energy Agency (IEA) (2026) *Global Energy Review 2026*. Paris: IEA. Available at: https://www.iea.org/reports/global-energy-review-2026 (Accessed: 11 July 2026).
[18] Forman, C., Muritala, I.K., Pardemann, R. and Meyer, B. (2016) 'Estimating the global waste heat potential', *Renewable and Sustainable Energy Reviews*, 57, pp. 1568–1579. doi:10.1016/j.rser.2015.12.192.
[19] Firth, A., Zhang, B. and Yang, A. (2019) 'Quantification of global waste heat and its environmental effects', *Applied Energy*, 235, pp. 1314–1334. doi:10.1016/j.apenergy.2018.10.102.

2.2 Temperature quality

A central feature of the world resource is its low temperature. Forman et al. estimated that about 63% of considered streams were below 100°C.[20] The independent exergy compilation by Bohra and Vitta divided 69.1 EJ of global waste-heat exergy into:

Temperature band	Estimated exergy	Share of estimated exergy	Typical sources
Below 100°C	30.5 EJ	44%	condensers, cooling water, data centres, refrigeration, wastewater, building cooling
100–300°C	14.4 EJ	21%	dryers, kilns, engine exhaust after treatment, food and paper processes
Above 300°C	24.1 EJ	35%	furnaces, steel, cement clinker, glass, metal smelting, turbine exhausts

These exergy numbers are theoretical and derive from a preprint rather than a harmonised international statistical system.[21] They nevertheless illustrate why a smaller high-temperature stream can be more valuable than a much larger near-ambient stream. Figure 2 presents the temperature-band distribution reported above.

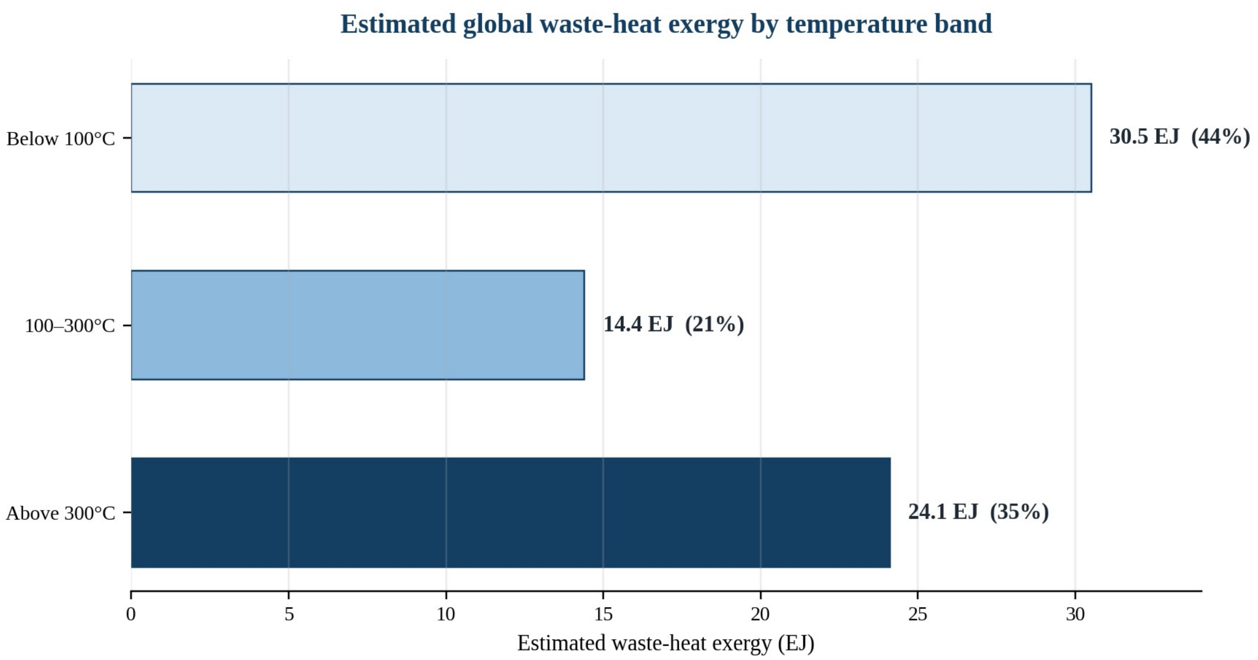

Figure 2. Estimated global waste-heat exergy by temperature band.

[20] Forman, C., Muritala, I.K., Pardemann, R. and Meyer, B. (2016) 'Estimating the global waste heat potential', *Renewable and Sustainable Energy Reviews*, 57, pp. 1568–1579. doi:10.1016/j.rser.2015.12.192.
[21] Bohra, A. and Vitta, S. (2022) 'Sustainability of large scale waste heat harvesting using thermoelectric', arXiv:2208.00616. Available at: https://arxiv.org/abs/2208.00616 (Accessed: 11 July 2026).

2.3 Major global source categories

Source category	Present significance	Typical temperature	Main recovery routes	Expected direction
Thermal electricity generation	Largest concentrated low-grade source in coal, gas and nuclear systems	20–50°C cooling water; 80–180°C stack gas	district heat, absorption cooling, heat pumps, condenser integration	Declines in strong renewable scenarios; persists in fossil, nuclear, biomass and CCS systems
Transport using combustion engines	Very large and highly dispersed	80–700°C coolant and exhaust	turbo-compounding, thermoelectrics, onboard heating; limited external reuse	Declines as electric vehicles expand
Iron and steel	High-quality industrial source	200–1,500°C	gas recovery, coke dry quenching, steam/power, storage, process preheat	Output grows in emerging economies; process route shifts alter heat profile
Cement and lime	Continuous, high-temperature exhaust	250–400°C kiln/preheater streams	waste-heat boilers, ORC, raw-material drying	Production grows in developing regions; efficiency lowers heat per tonne
Chemicals, petrochemicals and refining	Large, diverse and continuous	80–800°C	pinch integration, steam networks, heat pumps, ORC	Remains large; product mix and electrification change temperature levels
Pulp, paper, food and beverages	Medium/low temperature and steam-rich	40–250°C	condensate recovery, heat pumps, drying and hot-water reuse	Grows with production; favourable for onsite cascading
Buildings and air conditioning	Diffuse but rapidly rising	25–50°C	heat-recovery chillers, ambient loops, district energy	Strong growth in hot and urbanising regions
Data centres	Concentrated, predictable low-grade heat	25–60°C, higher with liquid cooling	heat pumps, district heating, hot-water use	More than doubles to 2030 in IEA base case
Wastewater and sewer systems	Stable urban low-grade source	10–30°C	water-source heat pumps	Increases with urbanisation and network deployment
Oil and gas flaring	Wasted fuel rather than conventional downstream heat	flame temperatures >1,000°C	eliminate flare, capture gas, power/heat production	Policy target is elimination, but volumes increased through 2025

Figure 3 summarises the indicative relationship between source temperature and the principal recovery pathways listed above.

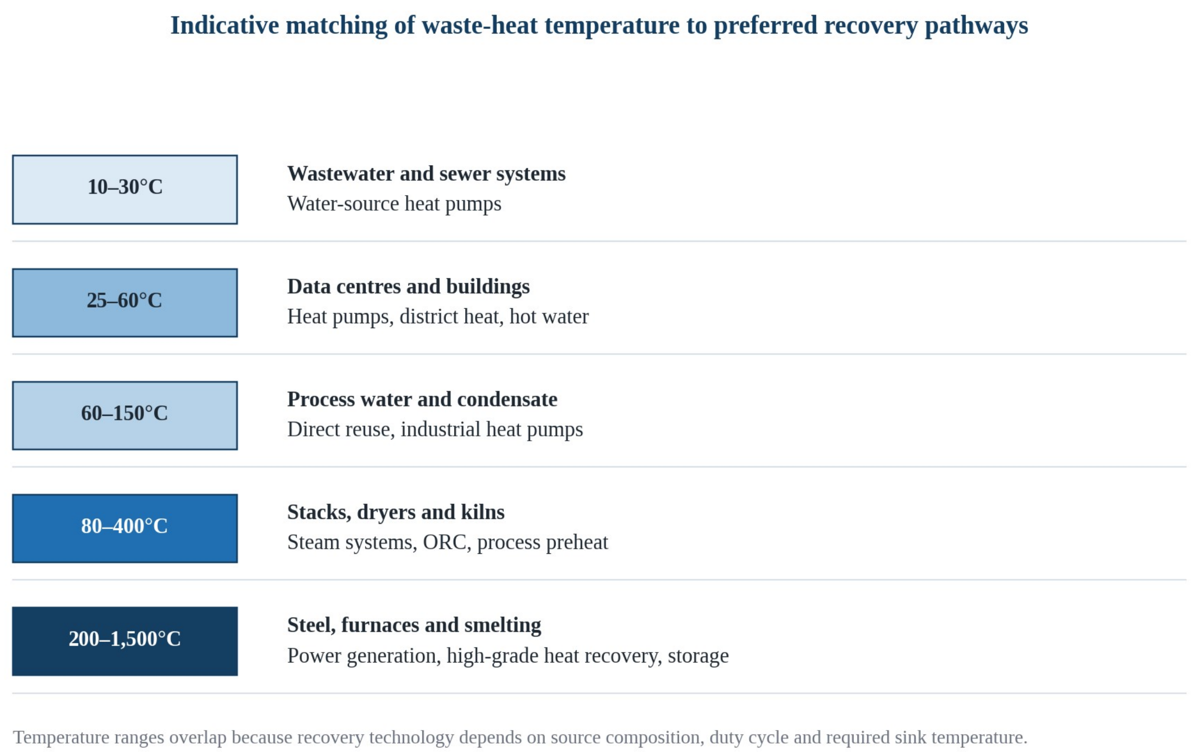

Figure 3. Indicative matching of source temperature to preferred recovery pathways. The ranges overlap, and the appropriate technology remains site-specific.

3. Regional evidence and principal contributors

3.1 East Asia: China, Japan, Korea and Taiwan

China

China is the only major economy with a recent comprehensive national study. Liu et al. estimated approximately 50 EJ of human-activity waste heat in 2021. About 40.6 EJ (81%) was below 50°C, making heat pumps, low-temperature networks and direct heating more relevant than electricity generation for most of the physical resource.[22]

The earlier societal accounting model for 2018 found waste heat equal to 42% of primary energy input. Electricity generation contributed 45% of the total, and 88% of power-sector heat was below 100°C. Low-temperature heat below 100°C represented 66% of all waste heat, while industrial heat was predominantly above 300°C and had the highest work potential.[23]

Northern China illustrates spatially useful recovery. Luo et al. estimated that about 100 Mtce, or 2.93 EJ, of low-grade industrial waste heat could be recovered during the heating season, together with major water savings.[24]

[22] Liu, Z., Yang, X., Sun, D. and Xia, J. (2026) 'Assessment of waste heat in China: Characteristics and national potential', *Energy*, 344, 139860. doi:10.1016/j.energy.2025.139860.
[23] Lin, Y., Chong, C.H., Ma, L., Li, Z. and Ni, W. (2022) 'Quantification of waste heat potential in China: A top-down Societal Waste Heat Accounting Model', *Energy*, 261, 125194. doi:10.1016/j.energy.2022.125194.
[24] Luo, A., Fang, H., Xia, J., Lin, B. and Jiang, Y. (2017) 'Mapping potentials of low-grade industrial waste heat in Northern China', *Resources, Conservation and Recycling*, 125, pp. 335–348. doi:10.1016/j.resconrec.2017.06.018.

Major Chinese contributors

1. Coal-fired and other thermal power plants, especially condenser and cooling-water heat.
1. Iron and steel clusters in Hebei, Jiangsu, Shandong, Liaoning and other industrial provinces.
2. Cement, chemicals, petrochemicals, coking, non-ferrous metals and glass.
3. Urban wastewater-treatment plants and sewer networks.
4. Data centres concentrated around major digital and power hubs.
5. District-heating plants and combined heat-and-power systems where return temperatures remain high.

Japan and South Korea

No equally recent whole-economy inventory was found. Their major sources are thermal power, steel, petrochemicals, refineries, cement, automotive manufacturing and high-density data centres. The value is concentrated in large coastal industrial complexes where heat integration and district-energy opportunities are spatially favourable. Continued nuclear operation also produces large low-grade condenser streams, while renewable growth reduces fossil condenser heat.

Taiwan

A bottom-up study of more than 11,000 industrial boilers estimated a theoretical industrial waste-heat potential of 89.66 PJ/year above 35°C and a technical potential of 6.92 PJ/year above 150°C.[25] Petrochemicals, electronics manufacturing, metals and power generation are the principal clusters.

3.2 South Asia: India and neighbouring economies

India's industrial growth makes it one of the most important future waste-heat regions, but national data remain fragmented. Saha, Chakraborty and Dutta assessed iron and steel, chemicals and petrochemicals, pulp and paper, cement and glass. Their modelling identified chemicals and petrochemicals as having the greatest theoretical waste-heat-to-power capacity, while iron and steel delivered the largest economically screened ORC power potential, up to 66.5 TWh under the study assumptions.[26]

A new market assessment commissioned by Energy Efficiency Services Limited under a UNEP/GEF programme confirms that substantial untapped heat remains across Indian industry and identifies the need for standardised audits, project aggregation and financing.[27]

Major South Asian contributors

1. Integrated iron and steel plants and sponge-iron/direct-reduction facilities in India.
1. Cement kilns in India, Pakistan and Bangladesh.
2. Refineries, fertiliser and petrochemical complexes.
3. Coal-fired power generation.
4. Pulp and paper, sugar, distilleries, textiles, glass, ceramics and food processing.

---

[25] Hong, G.B., Pan, T.C., Chan, D.Y.L. and Liu, I.H. (2020) 'Bottom-up analysis of industrial waste heat potential in Taiwan', *Energy*, 198, 117317. doi:10.1016/j.energy.2020.117317.

[26] Saha, B.K., Chakraborty, B. and Dutta, R. (2020) 'Estimation of waste heat and its recovery potential from energy-intensive industries', *Clean Technologies and Environmental Policy*, 22, pp. 1795–1814. doi:10.1007/s10098-020-01919-7.

[27] International Institute for Energy Conservation (IIEC), Energy Efficiency Services Limited and United Nations Environment Programme (2026) *Market Assessment of Waste Heat Recovery Solutions in India*. Available at: https://www.iiec.org/library/iiec-knowledge-products/papers-studies-reports/953-market-assessment-of-waste-heat-recovery-solutions-in-india (Accessed: 11 July 2026).

5. Brick kilns and small and medium enterprises, whose resource is large in aggregate but difficult to finance.

India's waste-heat amount is expected to increase in absolute terms as steel, cement, chemicals and data-centre activity grow. Heat per unit of output should fall with best-available equipment, greater internal heat recovery, electrification and process redesign.

3.3 Europe

Europe has the strongest geospatial evidence for matching industrial sources to heat demand. Manz et al. mapped 1,608 energy-intensive sites in EU-27 plus the United Kingdom. Cooling exhaust gases to 25°C yielded 960 PJ/year (267 TWh/year). Forty-seven per cent of sites were inside or within 10 km of district-heating areas. About 230 PJ/year (64 TWh/year) was available to current district-heating areas; future low-temperature networks increased deliverable heat to 258 PJ/year at 55°C or 679 PJ/year at 25°C.[28]

The principal industrial sources close to existing heat networks were refineries, cement kilns and blast furnaces. The wider list includes chemicals, paper, glass, non-ferrous metals, food processing and waste incineration. Urban source, data centres, wastewater treatment, metro systems, refrigeration and large buildings, are lower temperature but often closer to demand. European research estimated that urban waste heat could meet more than 10% of heat and hot-water demand if networks and heat pumps were deployed.[29]

Major European country and cluster contributors

- Germany: chemicals, refineries, steel, cement, glass and dense industrial regions such as North Rhine-Westphalia.
- France: nuclear and thermal condenser heat, refineries, chemicals, steel, cement and food processing.
- Italy and Spain: refineries, cement, ceramics, steel, glass and food industries.
- Poland, Czechia and other Central European systems: coal power, district heating, steel, cement and chemicals.
- Netherlands and Belgium: refineries, petrochemicals, ports, greenhouses and dense heat-demand corridors.
- United Kingdom: refineries, chemicals, steel, cement, food, wastewater and rapidly expanding data centres.
- Nordic countries: pulp and paper, metals, refineries, data centres and strong district-heating integration.

Europe's total industrial heat resource is likely to decline per tonne as industrial efficiency improves and blast-furnace steel is replaced by electric or hydrogen routes. At the same time, the technically useful share can rise because fourth- and fifth-generation heat networks accept lower temperatures and large heat pumps make 20–80°C sources usable.

[28] Manz, P., Kermeli, K., Persson, U., Neuwirth, M., Fleiter, T. and Crijns-Graus, W. (2021) 'Decarbonizing district heating in EU-27 + UK: How much excess heat is available from industrial sites?', *Sustainability*, 13(3), 1439. doi:10.3390/su13031439.
[29] Wheatcroft, E., Wynn, H., Lygnerud, K. and Bonvicini, G. (2020) 'The role of low temperature waste heat recovery in achieving 2050 goals: A policy positioning paper', *Energies*, 13(8), 2107. doi:10.3390/en13082107.

Figure 4 illustrates the European network-access quantities reported in this section.

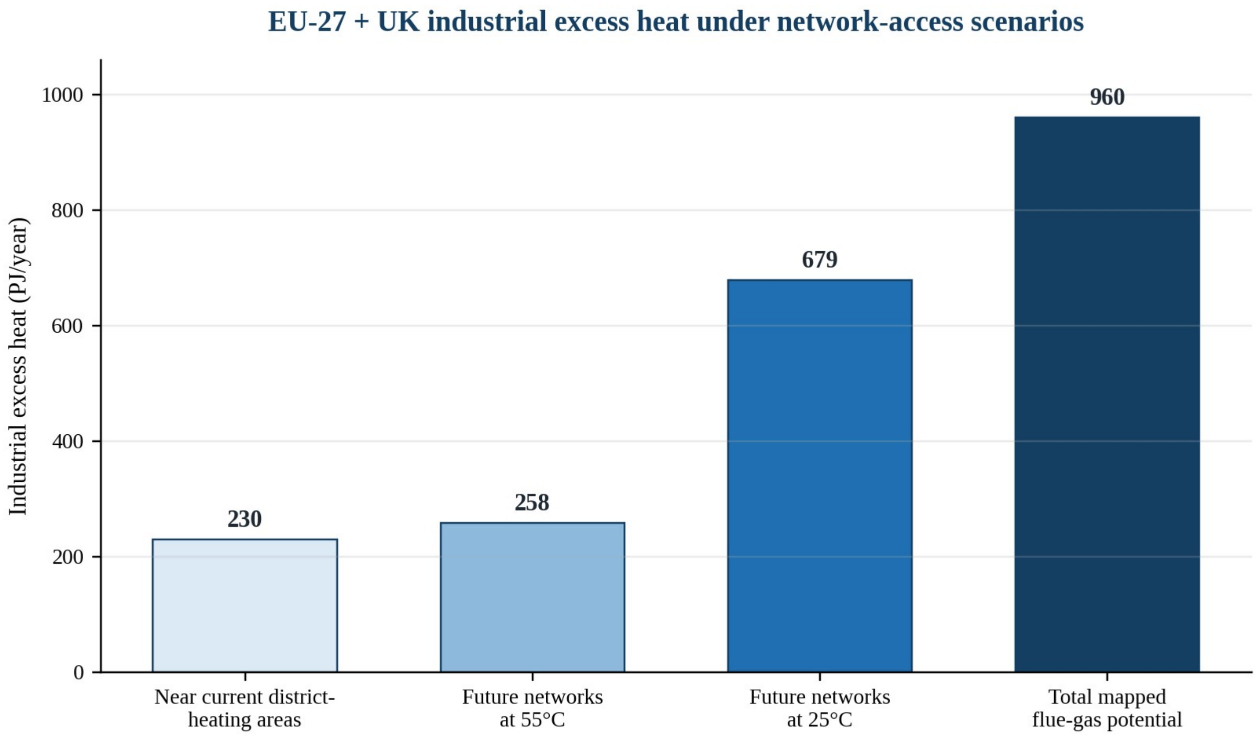

Figure 4. EU-27 plus the United Kingdom industrial excess heat under current and future network-access scenarios.

3.4 North America

United States

The 2023 LLNL flow chart reports 93.7 quads of total energy consumption, 61.57 quads of rejected energy and 32.1 quads of energy services.[30] The rejected-energy quantity is approximately 65 EJ and includes power-generation losses, vehicle losses, building conversion losses and industrial losses. It is a broad efficiency indicator rather than a heat-recovery inventory.

DOE states that 20–50% of industrial energy input is lost as hot exhaust gas, cooling water, equipment-surface heat and heated products.[31] Earlier bottom-up United States studies assessed eight energy-intensive sectors responsible for roughly 80% of industrial energy use and estimated 1,501–1,583 PJ/year of industrial waste heat.[32] Although dated, the sector ranking remains useful.

Major United States contributors

1. Electricity generation, particularly steam-cycle condenser heat.
1. Road transport, where most fuel energy is rejected by engines and brakes.
2. Chemicals and petroleum refining.

---

[30] Lawrence Livermore National Laboratory (LLNL) (2026) *Estimated U.S. Energy Consumption in 2023: 93.7 Quads*. Livermore, CA: LLNL. Available at: https://flowcharts.llnl.gov/commodities/energy (Accessed: 11 July 2026).
[31] U.S. Department of Energy (2026) 'Waste Heat Recovery Basics'. Washington, DC: DOE. Available at: https://www.energy.gov/cmei/ito/waste-heat-recovery-basics (Accessed: 11 July 2026).
[32] Miró, L., Brückner, S. and Cabeza, L.F. (2015) 'Mapping and discussing industrial waste heat potentials for different countries', *Renewable and Sustainable Energy Reviews*, 51, pp. 847–855. doi:10.1016/j.rser.2015.06.035.

3. Forest products and pulp and paper.
4. Iron and steel, foundries and aluminium.
5. Cement, lime, glass and other non-metallic minerals.
6. Food and beverage processing and industrial refrigeration.
7. Data centres, with rapid expansion in Virginia, Texas, Oregon, the Midwest and other grid hubs.

Canada and Mexico

Canada's major concentrated sources are oil sands upgrading, refineries, natural-gas processing, pulp and paper, mining and smelting, steel, cement and thermal power. Older literature reported 2,300 PJ/year of industrial waste heat, but the source boundaries were insufficiently clear and the international review considered the value unusually high; it should not be treated as a contemporary inventory.[33]

Mexico's principal sources are oil refining, petrochemicals, gas processing, cement, steel, glass, food processing, thermal power and flaring. Mexico was one of the nine largest flaring countries in 2024 and 2025.[34]

3.5 Middle East and North Africa

MENA's waste-heat profile is shaped by fossil electricity, hydrocarbons and water production. In 2024, natural gas supplied 70% of regional electricity; oil-fired generation remained especially important in Iraq, Saudi Arabia and Kuwait. Gas-fired capacity is expected to account for 20% of global gas-power investment to 2035.[35]

Major contributors by country and activity

- Saudi Arabia: oil- and gas-fired power, refineries, petrochemicals, gas processing, cement, steel and thermal desalination.
- Iran: gas power, refineries, petrochemicals, steel, cement and large oilfield flaring.
- Iraq: oil-fired power, refineries, cement and very large flaring losses.
- UAE and Qatar: gas power, LNG, gas processing, aluminium, refineries, petrochemicals and desalination.
- Kuwait, Oman and Bahrain: oil/gas power, refining, petrochemicals, aluminium and desalination.
- Algeria, Libya and Egypt: gas power, LNG/gas processing, refining, fertiliser, cement and flaring.
- Turkey: steel, cement, glass, ceramics, refineries and thermal power.

Gas flaring is not the same as waste heat from an industrial outlet: it is fuel destroyed before useful conversion. Nevertheless, its energy scale is important. World Bank satellite analysis found 167 bcm flared globally in 2025, equivalent to roughly 6 EJ of natural-gas energy using a representative lower heating value. Russia, Iran, Iraq, Venezuela, Mexico, Libya, Algeria, Nigeria and the United

[33] Miró, L., Brückner, S. and Cabeza, L.F. (2015) 'Mapping and discussing industrial waste heat potentials for different countries', *Renewable and Sustainable Energy Reviews*, 51, pp. 847–855. doi:10.1016/j.rser.2015.06.035.
[34] World Bank (2026) *Global Gas Flaring Tracker Report 2026*. Washington, DC: World Bank. Available at: https://www.worldbank.org/en/programs/gasflaringreduction/publication/2026-global-gas-flaring-tracker-report (Accessed: 11 July 2026).
[35] International Energy Agency (IEA) (2025) *The Future of Electricity in the Middle East and North Africa*. Paris: IEA. Available at: https://www.iea.org/reports/the-future-of-electricity-in-the-middle-east-and-north-africa (Accessed: 11 July 2026).

States produced 83% of global flaring.[36] The highest-value action is to prevent flaring and use the gas, not to recover heat from the flame.

Future MENA waste heat will be influenced by conversion from thermal desalination to reverse osmosis, renewable electricity growth, continued gas generation, hydrogen and ammonia projects, and new data centres. Reverse osmosis reduces thermal-rejection intensity, while electrolysers, compressors and synthesis plants create new low- and medium-temperature streams.

3.6 Latin America and the Caribbean

No harmonised contemporary regional inventory was identified. The largest sources are concentrated in a limited number of industrial and extractive economies.

Major contributors

- Brazil: iron and steel, pulp and paper, alumina/aluminium, oil refining, petrochemicals, cement, sugar and ethanol, food processing and thermal power.
- Mexico: refining, petrochemicals, cement, steel, glass, automotive manufacturing, thermal power and flaring.
- Venezuela: oil production, upgrading/refining and flaring.
- Argentina: refining, petrochemicals, food processing, steel, cement and gas production.
- Chile and Peru: copper mining, smelting, mineral processing and desalination, plus cement.
- Colombia, Trinidad and Tobago and other hydrocarbon producers: refining, gas processing, fertiliser and petrochemicals.

A 2023 assessment reviewed waste-heat recovery in the six largest Latin American cement-producing countries, together representing 82% of regional cement output, confirming cement as a broadly distributed high-temperature opportunity.[37] The Inter-American Development Bank identifies aluminium, cement, pulp and paper, and steel as core sectors for regional industrial transformation.[38]

The regional total should rise with minerals processing, data centres and industrial output, but the composition will change as Brazil's renewable electricity, electrified mining and green-hydrogen projects replace combustion processes.

3.7 Sub-Saharan Africa

National inventories are particularly weak. Industrial sources are geographically concentrated, which can make site-specific projects attractive despite low regional totals.

Major contributors

1. South African coal power, refineries, steel, ferroalloys, mining and minerals processing, cement, pulp and paper and food production.
1. Nigerian oil and gas production, flaring, refineries, cement and fertiliser.
2. Angolan oil production and flaring.

---

[36] World Bank (2026) *Global Gas Flaring Tracker Report 2026*. Washington, DC: World Bank. Available at: https://www.worldbank.org/en/programs/gasflaringreduction/publication/2026-global-gas-flaring-tracker-report (Accessed: 11 July 2026).

[37] 'Potential savings in the cement industry using waste heat recovery technologies' (2023) *Energy*, article S0360544223012045. Available at: https://www.sciencedirect.com/science/article/pii/S0360544223012045 (Accessed: 11 July 2026).

[38] Inter-American Development Bank (2025) *Pathways to Accelerate Industrial Transformation in Latin America and the Caribbean: Focus on Aluminum, Cement, Pulp & Paper, and Steel*. Washington, DC: IDB. Available at: https://publications.iadb.org/en/pathways-accelerate-industrial-transformation-latin-america-and-caribbean-focus-aluminum-cement (Accessed: 11 July 2026).

3. Cement in Ethiopia, Kenya, Tanzania, Ghana, Senegal and other rapidly urbanising economies.
4. Copper and cobalt processing in Zambia and the Democratic Republic of the Congo.
5. Aluminium smelting in Mozambique and other power-intensive metals sites.
6. Diesel generation, cold chains and food processing across distributed systems.

Nigeria remained among the nine largest flaring countries in 2025.[39] South African research emphasises that inaccessible and inconsistent plant data remain a major barrier to robust national estimation.[40] A 2025 Ethiopian cement study demonstrates the potential for plant-level waste-heat power but does not provide a continent-wide total.[41]

Industrialisation and rising cooling demand will increase absolute heat rejection. Recovery priorities should focus on cement kilns, mineral furnaces, refineries, captive power and cold-chain systems where annual operating hours and avoided electricity costs are high.

3.8 Eurasia and Russia

Russia is a major global waste-energy contributor because of its large thermal-power system, metals industry, chemicals, refining, oil and gas production, district heating and flaring. It was the largest or one of the largest flaring countries in recent World Bank data.[42] Kazakhstan, Uzbekistan, Azerbaijan and other regional economies add thermal power, steel, non-ferrous metals, refining and gas processing.

The most valuable regional opportunities are reduction of flaring, modernisation of district-heating networks, refinery and chemical integration, metallurgical heat recovery and replacement of inefficient steam systems. Political and data-access constraints make current harmonised estimates uncertain.

3.9 Southeast Asia

Southeast Asia's industrial and electricity demand is growing rapidly. Major sources are coal and gas power, cement, steel, petrochemicals, oil refining, palm-oil and food processing, pulp and paper, electronics and data centres.

Major contributors

- Indonesia: coal power, cement, steel, refineries, nickel processing, pulp/paper and palm oil.
- Vietnam: coal power, cement, steel, textiles and electronics.
- Thailand: petrochemicals, refineries, cement, food processing, automotive manufacturing and data centres.
- Malaysia and Singapore: refining, petrochemicals, LNG, electronics and data centres.
- Philippines: coal/geothermal power, cement, food processing and electronics.

---

[39] World Bank (2026) *Global Gas Flaring Tracker Report 2026*. Washington, DC: World Bank. Available at: https://www.worldbank.org/en/programs/gasflaringreduction/publication/2026-global-gas-flaring-tracker-report (Accessed: 11 July 2026).
[40] University of the Witwatersrand (n.d.) *Energy-efficiency improvement study: A case study of waste heat recovery in selected manufacturing industries in Johannesburg*. Johannesburg: Wits University. Available at: https://wiredspace.wits.ac.za/items/111b9159-df7e-4240-bce7-803d8d9df393 (Accessed: 11 July 2026).
[41] 'Techno-economic analysis of waste heat recovery power plants in cement industry – A case study in Ethiopia' (2025) *Next Energy*, 100339. doi:10.1016/j.nxener.2025.100339.
[42] World Bank (2026) *Global Gas Flaring Tracker Report 2026*. Washington, DC: World Bank. Available at: https://www.worldbank.org/en/programs/gasflaringreduction/publication/2026-global-gas-flaring-tracker-report (Accessed: 11 July 2026).

The IEA expects data-centre demand in Southeast Asia to more than double by 2030.[43] The regional resource will therefore shift toward a mixture of high-temperature heavy-industry heat and continuous low-grade digital-infrastructure heat.

3.10 Oceania

Australia's major sources are coal- and gas-fired power, LNG liquefaction and compression, alumina refining and aluminium smelting, iron and steel, mining and mineral processing, cement, chemicals, food processing and data centres. New Zealand's sources include pulp and paper, dairy and food processing, geothermal and thermal-power condensers, wood processing and wastewater.

No recent whole-economy waste-heat inventory was identified. Project development should use National Greenhouse and Energy Reporting data, site energy balances and industrial-cluster mapping rather than applying overseas percentages without adjustment.

4. Regional comparison table

Region	Best quantified contemporary evidence	Major source leaders	Confidence and boundary
World	Indicative gross heat approximately 320 EJ/year from 52% of approximately 623 EJ input; 69.1 EJ exergy estimate	power generation, transport, industry, buildings	Medium for global order of magnitude; low for recoverable amount
China	50 EJ in 2021; 81% below 50°C	power plants, steel, cement, chemicals, wastewater, data centres	High relative to other national inventories; study-model dependent
United States	65 EJ rejected energy in 2023; 1.5–1.6 EJ/year older industrial estimate	power, transport, chemicals/refining, forest products, metals, cement, data centres	High for rejected-energy accounting; medium/low for recoverable industrial heat
EU-27 + UK	0.96 EJ/year industrial flue-gas potential to 25°C; 0.23 EJ/year near current DH areas	refineries, cement, blast furnaces, chemicals, paper, glass	High for included sites and flue-gas boundary; excludes many low-grade sources
India	No comparable total; sector model identifies up to 66.5 TWh steel ORC potential	steel, chemicals, cement, thermal power, refineries, pulp/paper, glass	Medium for sector screening; low for national total
Taiwan	89.66 PJ/year theoretical >35°C; 6.92 PJ/year technical >150°C	boilers, petrochemicals, electronics, metals	Good bottom-up boiler coverage; limited source classes
MENA	No harmonised heat total; 167 bcm global flaring in 2025 with several MENA top contributors	power, refining, petrochemicals, LNG, desalination, flaring	High for flaring; low for conventional waste-heat total
Latin America	No harmonised total	refining, mining/smelting, steel, cement, pulp/paper, aluminium, food	Low regional quantification; strong sector evidence
Sub-Saharan Africa	No harmonised total	South African	Low regional quantification

[43] International Energy Agency (IEA) (2025) *Energy and AI*. Paris: IEA. Available at: https://www.iea.org/reports/energy-and-ai (Accessed: 11 July 2026).

Region	Best quantified contemporary evidence	Major source leaders	Confidence and boundary
		power/metals, Nigerian flaring/refining, cement, mining	
Oceania	No harmonised total	thermal power, LNG, alumina/aluminium, mining, steel, cement, food, data centres	Low national quantification

Figure 5 visualises selected quantified regional evidence while preserving the differing source boundaries described in the table.

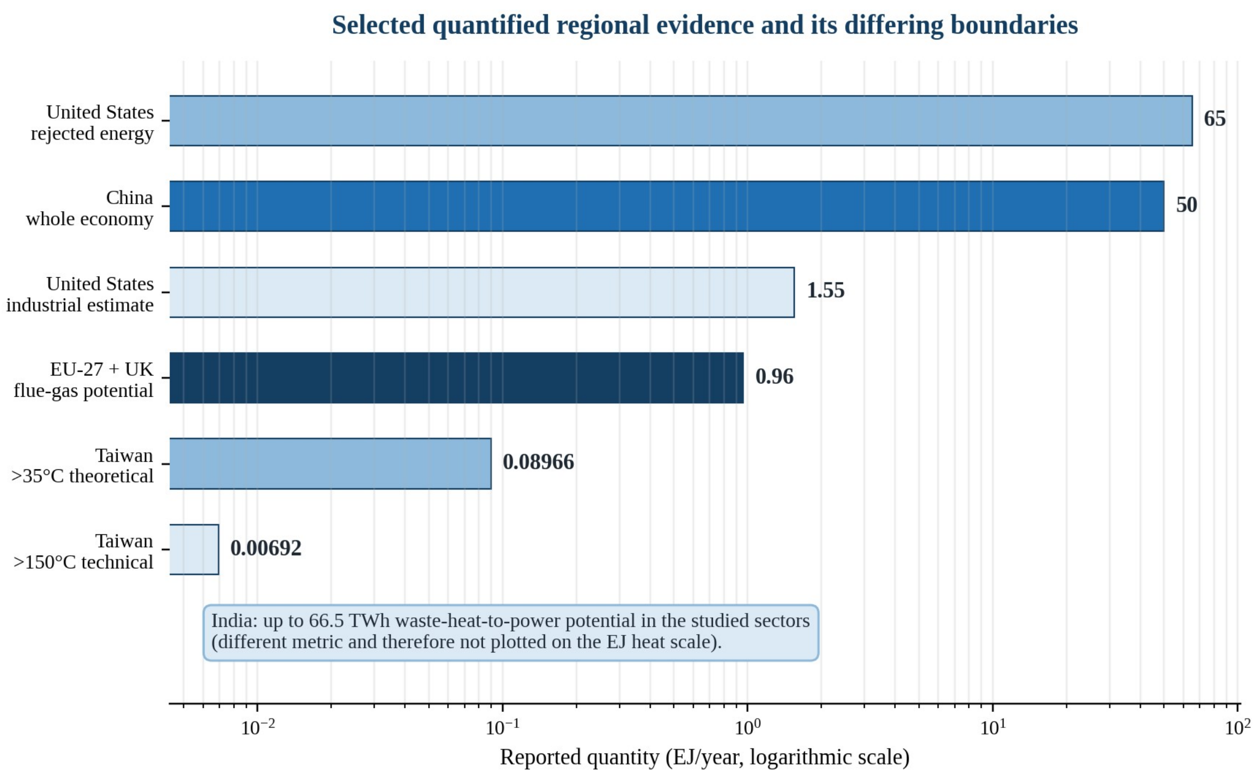

Figure 5. Selected quantified regional evidence. Values use different source boundaries and should not be summed or treated as directly comparable.

5. Future expectations to 2030 and 2050

5.1 Thermal power

The largest present low-grade source like thermal power condenser heat, will fall where coal and gas generation are displaced by wind and solar. It will not disappear. Nuclear, geothermal, biomass, waste-to-energy, gas balancing plants and fossil facilities with carbon capture still reject substantial heat. Carbon capture generally increases steam and cooling requirements, and Firth et al. found that CCS can increase thermal waste even while reducing climate forcing from carbon dioxide.[44]

Regional consequences differ. Europe and parts of North America should experience declining fossil condenser heat. China and India may retain large absolute streams during the transition even as their shares decline. MENA is projected to continue investing in gas generation through 2035.[45]

5.2 Transport electrification

Combustion vehicles reject most fuel energy through exhaust, coolant, friction and braking. Electric vehicles use much less energy per kilometre and recover some braking energy, so transport waste heat should decline in high-electrification scenarios. Firth et al. estimated that a 10% increase in electric-vehicle penetration reduced global waste heat in liquid and gaseous streams by 0.7–2.0% in their model.[46]

A remaining heat source will be battery, motor, power-electronics and fast-charging cooling, but it is much smaller than the avoided engine heat and usually lower temperature.

5.3 Data centres and artificial intelligence

Data centres are the clearest rapidly growing concentrated source. IEA estimates electricity use of about 415 TWh in 2024 and 945 TWh in 2030, equivalent to an increase from about 1.5 EJ to 3.4 EJ/year. Almost all site electricity eventually becomes heat, although the recoverable temperature and quantity depend on power-usage effectiveness, cooling technology and whether heat pumps are used.[47]

The United States and China account for about 80% of projected global growth to 2030. Europe grows more slowly in absolute terms but has strong district-heating opportunities. Southeast Asian demand more than doubles, although hot climates reduce space-heating sinks. Liquid cooling can raise outlet-water temperature and make heat recovery more useful than conventional air cooling.

Figure 6 shows the projected increase in data-centre electricity use and the associated scale of heat rejection.

5.4 Air conditioning and refrigeration

IEA projects the global building air-conditioner stock to rise from 1.6 billion to 5.6 billion units by 2050, with electricity demand tripling without stronger efficiency standards.[48] Every cooling system moves indoor heat outdoors and adds compressor electricity as heat. This will make urban heat rejection a major future stream, especially in China, India, Southeast Asia, MENA, Africa and Latin America.

Recovery is most attractive in facilities with simultaneous heating and cooling demand such as hospitals, hotels, food plants, supermarkets, campuses and mixed-use districts. In hot climates without a heat sink, the priority is efficiency, thermal storage and reduction of urban heat-island effects rather than heat recovery.

Figure 7 summarises the global cooling-growth indicators described above.

---

[44] Firth, A., Zhang, B. and Yang, A. (2019) 'Quantification of global waste heat and its environmental effects', *Applied Energy*, 235, pp. 1314–1334. doi:10.1016/j.apenergy.2018.10.102.

[45] International Energy Agency (IEA) (2025) *The Future of Electricity in the Middle East and North Africa*. Paris: IEA. Available at: https://www.iea.org/reports/the-future-of-electricity-in-the-middle-east-and-north-africa (Accessed: 11 July 2026).

[46] Firth, A., Zhang, B. and Yang, A. (2019) 'Quantification of global waste heat and its environmental effects', *Applied Energy*, 235, pp. 1314–1334. doi:10.1016/j.apenergy.2018.10.102.

[47] International Energy Agency (IEA) (2025) *Energy and AI*. Paris: IEA. Available at: https://www.iea.org/reports/energy-and-ai (Accessed: 11 July 2026).

[48] International Energy Agency (IEA) (2018) *The Future of Cooling*. Paris: IEA. Available at: https://www.iea.org/reports/the-future-of-cooling (Accessed: 11 July 2026).

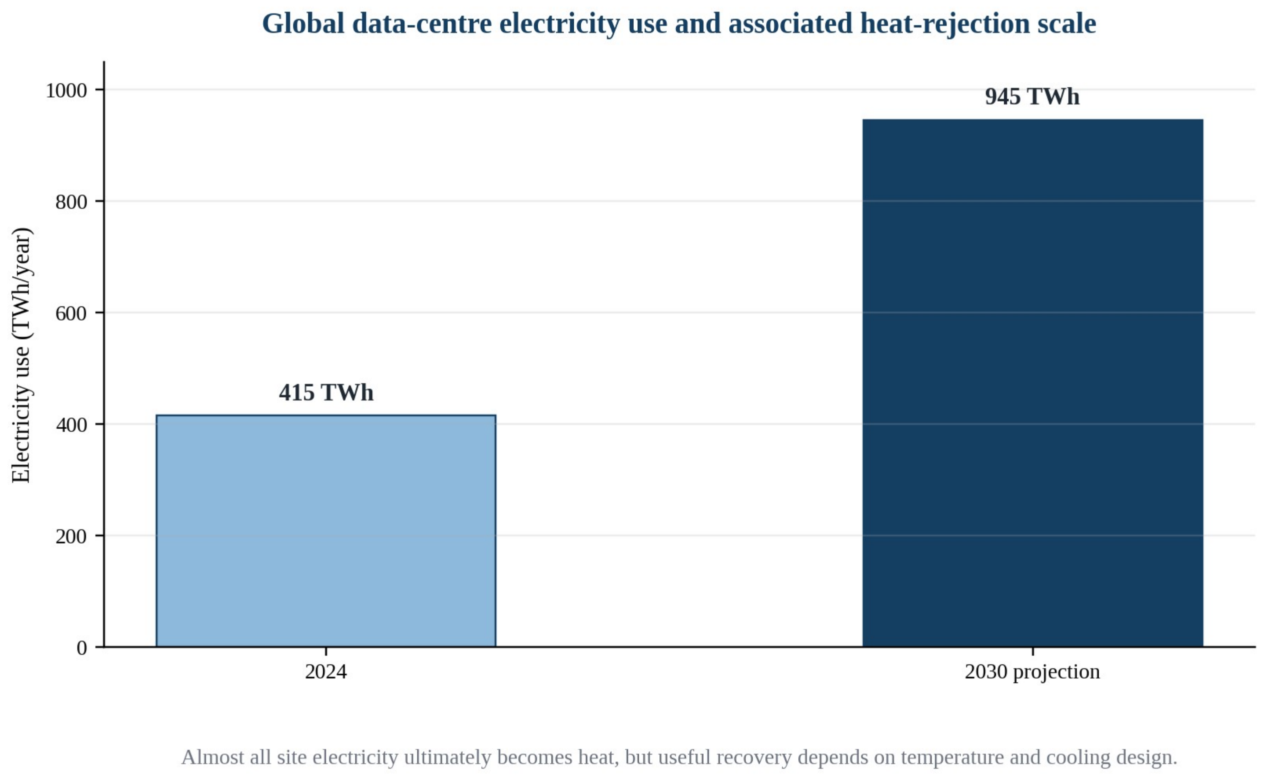

Figure 6. Global data-centre electricity use in 2024 and the IEA projection for 2030, indicating the scale of associated low-temperature heat rejection.

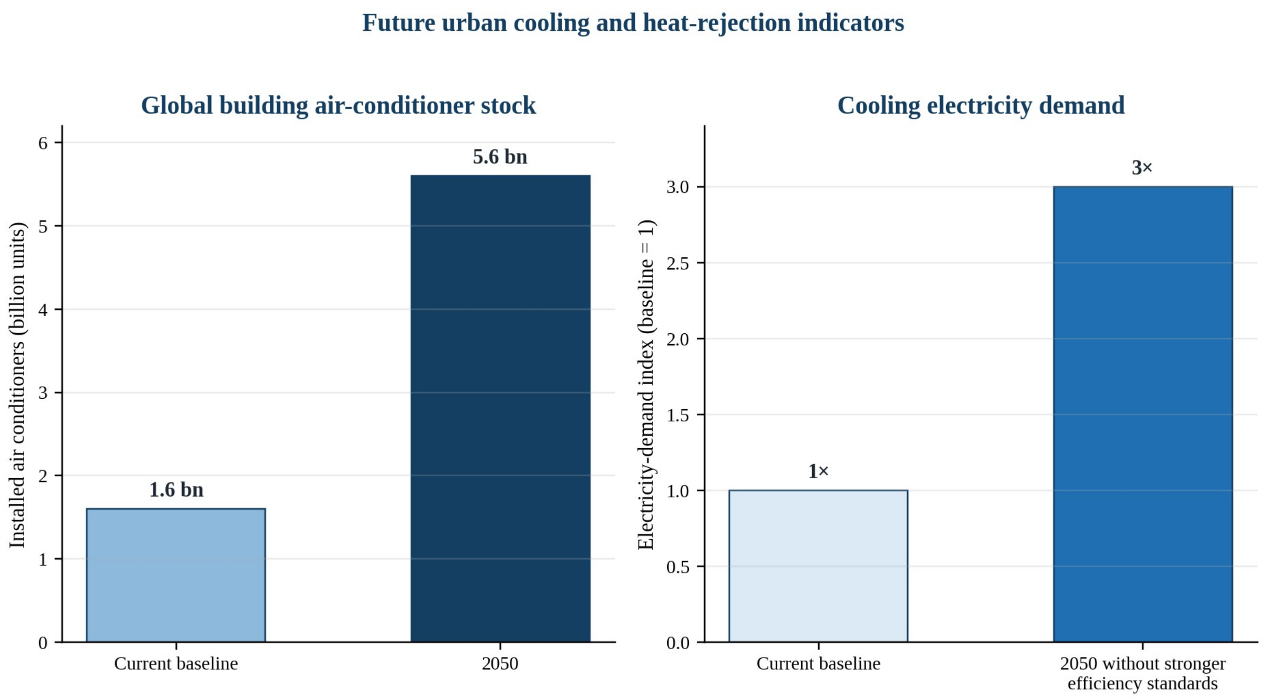

Figure 7. Global building air-conditioner stock and cooling-electricity-demand growth indicators to 2050.

5.5 Hydrogen, electrolysis and synthetic fuels

Electrolysers and downstream compressors, ammonia synthesis, methanol and e-fuel plants reject low- and medium-temperature heat. Installed global electrolysis capacity exceeded 4 GW in 2025, and the announced pipeline is much larger, although the IEA warns that more than 100 GW could miss 2030 without investment decisions.[49] Low-emissions hydrogen projects could produce 37 Mt/year by 2030 if announced projects materialise, but committed volumes are far smaller.[50]

Future hydrogen hubs in China, Europe, MENA, Australia, India, Chile and Namibia could become important heat sources. Recovery prospects improve where electrolysers are co-located with district heat, desalination, industrial drying or low-temperature processes.

5.6 Industrial transformation

Industrial electrification reduces combustion flue gas but does not eliminate heat rejection. Electric arc furnaces, resistance and induction heating, plasma, electrolysis and high-temperature heat pumps produce different waste streams. Green steel reduces coke-oven and blast-furnace gas but creates heat from direct-reduction gas cooling, hydrogen compression and electric furnaces. Cement efficiency and alternative binders lower heat per tonne, but global construction growth may keep absolute heat high.

In emerging Asia and Africa, production growth may exceed efficiency gains through 2030. In Europe, Japan and parts of North America, structural change and process efficiency are more likely to reduce gross high-temperature waste heat while increasing the relative importance of low-grade sources.

5.7 District heat, industrial heat pumps and thermal storage

Recovery technology expands the usable fraction even if gross waste heat falls. Low-temperature district systems can accept heat at 30–70°C, compared with older networks requiring much higher supply temperatures. Large heat pumps can upgrade 15–80°C sources to industrial or building temperatures. Thermal storage separates source availability from heat demand.

The EU industrial mapping demonstrates this effect: spatially deliverable industrial heat rises from 230 PJ/year around today's networks to as much as 679 PJ/year in a future low-temperature-network case, without assuming a larger gross industrial source.[51]

6. Investment and policy priorities

6.1 Patent-relevant operating and deployment conditions

The patented system should be evaluated first against continuous or high-duty gas streams whose conditions fall within, or can be efficiently brought within, the simulator's favourable operating region. The broad modelled region is approximately 350–430 K, corresponding to 77–157°C, at low relative humidity, absolute pressure around 120–180 kPa and available gas velocity around 25–45 m/s. The best-found comparative point occurred at approximately 145.9°C, 142.2 kPa absolute pressure, 45 m/s and 0% relative humidity.

These figures define an engineering screening window rather than universal operating limits. Temperature alone is insufficient. A source must also provide a suitable moving gas stream,

[49] International Energy Agency (IEA) (2026) *Global Hydrogen Review 2026: Production*. Paris: IEA. Available at: https://www.iea.org/reports/global-hydrogen-review-2026/production (Accessed: 11 July 2026).

[50] International Energy Agency (IEA) (2025) *Global Hydrogen Review 2025*. Paris: IEA. Available at: https://www.iea.org/reports/global-hydrogen-review-2025 (Accessed: 11 July 2026).

[51] Manz, P., Kermeli, K., Persson, U., Neuwirth, M., Fleiter, T. and Crijns-Graus, W. (2021) 'Decarbonizing district heating in EU-27 + UK: How much excess heat is available from industrial sites?', *Sustainability*, 13(3), 1439. doi:10.3390/su13031439.

adequate pressure and mass flow, low or manageable moisture content, sufficient annual operating hours, practical access for liquid injection and downstream flow control, and an economically useful connection to electrical equipment or onsite demand.

Within the focused optimal-input region, the simulated mean and median net-power increases exceeded 12%, with a maximum reported increase of 19.27%. These results support prioritising sources that naturally approach the favourable conditions rather than imposing energy-intensive conditioning on unsuitable streams.

6.2 Highest-priority source classes

Continuous, dry or dehumidifiable industrial gas exhaust within the favourable temperature range:

The strongest initial candidates are process gases from chemicals and petrochemicals, refineries, metals processing, industrial dryers, glass production, selected furnace exhausts and turbine or engine exhaust streams after upstream heat recovery. Preference should be given to sites with stable flow, moderate positive pressure and onsite electricity demand.

Hotter industrial exhaust capable of energy-preserving conditioning:

Steel, cement, smelting, high-temperature furnaces and kiln systems commonly discharge above the simulator’s preferred inlet range. These sources may remain suitable where high-grade heat is first recovered for process use, steam or conventional power generation and the remaining gas is then delivered to the patented system within the favourable range. Heat exchange, controlled blending, expansion recovery, parallel modules or increased flow area are preferable to dissipative throttling.

Medium-temperature streams requiring technology selection by physical form:

Gas streams between approximately 77°C and 157°C may be candidates for the patented system when pressure, velocity and humidity are suitable. Liquid water, condensate, low-velocity vapour and saturated process streams in the same temperature range will generally be better suited to direct reuse, heat exchangers or industrial heat pumps.

Low-temperature urban and industrial sources:

Data centres, wastewater, refrigeration, cooling water, buildings and metro systems remain important waste-heat resources, but their typical temperatures, pressures and flow forms generally place them outside the primary operating market for the patented turbine system. Their preferred recovery routes remain heat pumps, district-energy networks and direct heating.

Flaring and venting:

The first priority is to capture and use the fuel rather than recover heat from the flame. The patented system should be considered only for controlled downstream exhaust arising after useful combustion or process conversion, not as a substitute for flare elimination.

Thermal-power and industrial cluster applications:

Power stations, refineries, chemicals facilities, cement works and metals plants should be assessed at the level of individual exhaust trains. Plant surveys should record temperature, absolute pressure, velocity, humidity, composition, annual operating hours and existing upstream recovery before technical suitability is claimed.

6.3 Indicative patent-relevant global pool

The global exergy evidence identifies approximately 14.4 EJ/year between 100°C and 300°C. This is the closest published category to the simulator’s preferred temperature range, although it is substantially broader and does not report the other required inlet conditions.

For investment screening, applying a 10–25% compatibility factor to this medium-temperature exergy category gives an indicative patent-relevant candidate pool of approximately 1.44–3.60 EJ/year, or 400–1,000 TWh/year of exergy equivalent. The lower end represents selective deployment at naturally suitable sites; the upper end represents wider deployment with practical conditioning and modular integration.

7. Conclusions

The world releases waste heat on a scale of hundreds of exajoules per year, with a defensible gross order-of-magnitude estimate near 320 EJ/year. Only a fraction is technically or economically recoverable. Published global modelling places economic recovery at roughly 6–9% of energy input, while the available exergy study estimates approximately 69.1 EJ/year of theoretical useful-work potential. Of that exergy estimate, 30.5 EJ is below 100°C, 14.4 EJ is between 100°C and 300°C, and 24.1 EJ is above 300°C. These categories have different boundaries and should not be added to regional inventories as though they were directly comparable.

For the patented system, the total global waste-heat figure is less relevant than the quantity present as a continuous moving gas stream under suitable inlet conditions. The simulator identifies a broad favourable region around 350–430 K, low relative humidity, 120–180 kPa absolute pressure and 25–45 m/s, with the best-found result at 419 K, 142.2 kPa, 45 m/s and 0% relative humidity. The focused optimal-region simulations produced mean and median comparative net-power increases above 12%, while the best-found point produced a 19.27% increase over the otherwise identical dry configuration.

The closest quantified global proxy for this market is the 14.4 EJ/year medium-temperature exergy category between 100°C and 300°C. Because only part of that category will also satisfy the required gas form, humidity, pressure, velocity, operating continuity and integration conditions, a 10–25% compatibility screen gives an indicative patent-relevant pool of approximately 1.44–3.60 EJ/year, equivalent to approximately 400–1,000 TWh/year. This is a source-screening range, not a forecast of recovered electricity or commercial deployment. It deliberately excludes the unquantified upper portion of the below-100°C category and treats heat above 300°C as a secondary opportunity requiring energy-preserving upstream recovery or conditioning.

China remains the largest documented national waste-heat source, with approximately 50 EJ in 2021, although 81% was below 50°C and is therefore more relevant to heat pumps and heat networks than to the patented system. The United States records approximately 65 EJ of broad rejected energy, but that figure includes transport, conversion and low-temperature losses that are not directly addressable. Europe has the most mature industrial site mapping, with approximately 0.96 EJ/year of mapped flue-gas heat in the analysed sectors. India, MENA, Latin America, Africa, Southeast Asia and Oceania contain major steel, cement, refining, chemicals, metals and thermal-power clusters but lack harmonised inventories containing the operating variables needed for patent-specific screening.

The most promising commercial applications are therefore not the largest low-temperature heat sources. They are continuous industrial gas streams that naturally approach the favourable temperature, pressure, velocity and humidity range, or hotter streams that can pass through that range after useful upstream heat recovery. Chemicals, refineries, metals, glass, industrial drying, selected turbine exhausts, cement and steel facilities are the principal sectors for site-level assessment. Data centres, cooling water, wastewater and building heat remain important energy resources but generally require heat pumps or direct thermal networks rather than this system.

The strategic opportunity is consequently narrower than the approximately 320 EJ global headline but remains substantial. Commercial development should focus on identifying the compatible fraction of the estimated 1.44–3.60 EJ/year screening pool, validating performance with measured component data and demonstrating repeatable net electrical gains after pumps, auxiliaries, leakage and operating constraints are included. The simulator supports source selection and design optimisation, but prototype and industrial validation remain necessary before the modelled gains can be treated as realised energy recovery.

ANNEXURE C

US Patent 12,650,086 B1

Device for Conversion of Kinetic and Thermal Energies of Gas Flows to Work

Comparative-Energy Report

by Dr Benedict de St. Amatus
Solarius Technologies Pty Ltd (ABN: 83 667 177 353)
Queensland, Australia

2026

Executive summary

Annexure A reproduces the issued United States patent 12,650,086 B1: Device for Conversion of Kinetic and Thermal Energies of Gas Flows to Work, and its drawing, description and claims.

System configuration and operating principle:

The evaluated arrangement comprises a generating first turbine, an interstage water-injection zone and a downstream outlet-isolation rotor. Water is atomised immediately after Turbine 1; evaporation absorbs heat, changes the gas density and mass flow, and lowers the solved pressure in Zone 2. The outlet rotor controls forward discharge and helps limit reverse atmospheric-air ingress but receives no electrical-generation credit. Net electrical power is therefore the Turbine 1 electrical output less the pump and other auxiliary demands. The dry and injection-enabled cases use the same geometry and external conditions, with liquid flow set to zero in the dry case.

Objective:

A comprehensive mathematical model was used to identify inlet conditions that maximise the additional net electrical output obtained with water injection, compared with the same system operating dry. It also tested how inlet temperature, pressure, velocity and humidity affect performance.

Simulator:

The self-contained browser simulator is a quasi-steady, one-dimensional screening model. It combines humid-gas properties, droplet evaporation, Turbine 1 and outlet-rotor flow-capacity relations, pressure losses and a coupled mass-flow balance. For each operating scenario it solves Zone 2 pressure, checks pressure, temperature, evaporation, carryover, speed and flow constraints, optimises the common geometry and injection rate, and compares the injection-enabled result with the otherwise identical dry case.

Modelled favourable operating region:

Within the tested search space, positive comparative benefits were concentrated in warm, dry inlet gas. The strongest combined region occurred approximately between 350 and 430 K at low relative humidity, with favourable pressure and velocity combinations concentrated around 120-180 kPa(a) and 25-45 m/s. At the nominal values of the other inputs, the optimiser selected zero injection from approximately 50% RH upward. These ranges describe the tested configuration and are not universal design limits.

Notation:

T is absolute temperature, P is absolute pressure, v is available inlet velocity, RH is relative humidity, A is flow area, L is Zone 2 length, axial velocity v, D_{32} is the Sauter mean droplet diameter and Δ is the difference between the injection-enabled and dry cases. A_1 and A_2 denote the inlet/Zone 1 and Zone 2 flow areas, respectively. kPa(a) denotes absolute kilopascals; kW, MW and MWh denote kilowatts, megawatts and megawatt-hours.

Best comparative point found:

Within the tested search space, the strongest incremental result was obtained at T = 419 K (145.9 °C), P = 142.2 kPa(a), available inlet velocity v = 45.0 m/s and RH = 0.0%. With $A_1 = A_2 = 2.0\ m^2$, Zone 2 length 8.0 m, target droplet diameter 20 µm and liquid ratio 0.0393 kg/kg dry gas, the model returned 1.144 MW dry and 1.365 MW injected net power. The increase was 220.498 kW (19.27%), equivalent to 1.764 MWh over the eight-hour scenario.

The strongest interaction was temperature with humidity: warm, very dry inlet gas supported the largest evaporation-driven advantage. At nominal values of the other variables, the fine one-factor peaks were approximately 372 K for incremental power, 168 kPa(a) for incremental power, 34 m/s for incremental power and 4% RH for incremental power. High humidity progressively removed the benefit; at the nominal case the optimiser selected zero injection from approximately 50% RH upward. Pressure and velocity exhibit capacity- and constraint-driven discontinuities. The reported optimum is therefore a best-found point, not proof of a unique global optimum. When inlet conditions exceed the comparative optimum, conditioning should be by heat/enthalpy blending, dehumidification or dry-air blending, pressure let-down/expansion, and flow splitting or area increase - not by indiscriminate throttling that destroys recoverable energy.

Appendix C1 reproduces the corresponding simulator input, calculated results and embedded mathematical-model interface.

Figure 1 shows the dry and injection-enabled output at the best comparative point found.

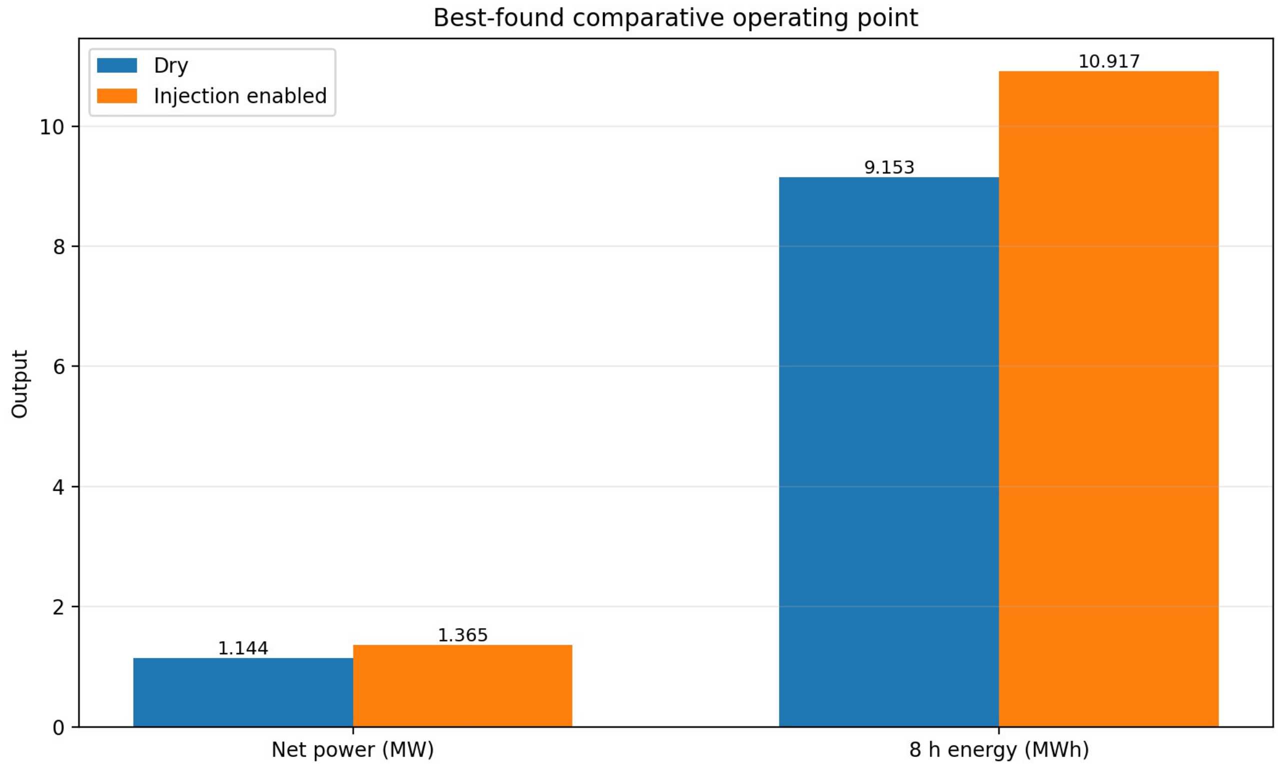

Figure 1. Dry and injection-enabled output at the best comparative point found.

Tested operating range and best comparative operating point

The inlet corresponds to Zone 1, immediately upstream of Turbine 1, where the specified temperature T, absolute pressure P, available axial velocity v and relative humidity RH define the incoming gas. Turbine 1 is the electrical-generating rotor. Zone 2 is the constant-area interstage region immediately downstream of Turbine 1 and upstream of the outlet-isolation rotor; it contains the water injector and provides the length L for droplet residence and evaporation. A_1 and A_2 are the inlet and Zone 2 flow areas and are equal in this evaluated case. D_{32} is the target Sauter mean droplet diameter. The outlet-isolation rotor regulates forward discharge and limits reverse atmospheric ingress without receiving electrical-generation credit. The tables below define the search envelope and report the best feasible paired dry-versus-injection result.

The simulator varied each inlet variable independently, examined all two-variable combinations, sampled the full four-variable operating space and then refined the strongest feasible region.

ANNEXURE C

US Patent 12,650,086 B1: Device for Conversion of Kinetic and Thermal Energies of Gas Flows to Work

Comparative-Energy Report

Variable	Broad tested range	Nominal held value
Inlet temperature	210-850 K	333.15 K
Inlet absolute pressure	105-500 kPa(a)	125 kPa(a)
Available inlet velocity	5-200 m/s	35 m/s
Inlet relative humidity	0-100%	20%
Ambient pressure / temperature / RH	Fixed	101.325 kPa(a) / 298.15 K / 50%
Operating duration	Fixed	8 h

Quantity	Dry case	Injection-enabled case	Change
Net electrical power	1.1441 MW	1.3646 MW	+220.5 kW
Eight-hour net energy	9.153 MWh	10.917 MWh	+1.764 MWh
Paired gain	-	-	19.27%
Turbine 1 electrical output	1.1444 MW	1.3670 MW	+222.5 kW
Pump demand	0	2.018 kW	-2.018 kW
Zone 2 pressure	122.807 kPa(a)	119.589 kPa(a)	-3218 Pa
Zone 2 temperature	133.42 °C	40.19 °C	-93.22 K

Input or design parameter	Best-found value
Inlet temperature	419 K (145.9 °C)
Inlet absolute pressure	142.2 kPa(a)
Available inlet velocity	45.0 m/s
Inlet relative humidity	0.0%
Common area $A_1 = A_2$	2.00 m²
Zone 2 length	8.00 m
Target droplet diameter	20 µm
Liquid/dry-gas ratio	0.03926 kg/kg
Liquid flow	4.010 kg/s
Calculated evaporation fraction	99.99998%
Calculated nozzle count	453
Eight-hour reservoir including simulator reserve factor	144.7 m³

Figure 2 shows the pressure and temperature profiles at the best comparative point found.

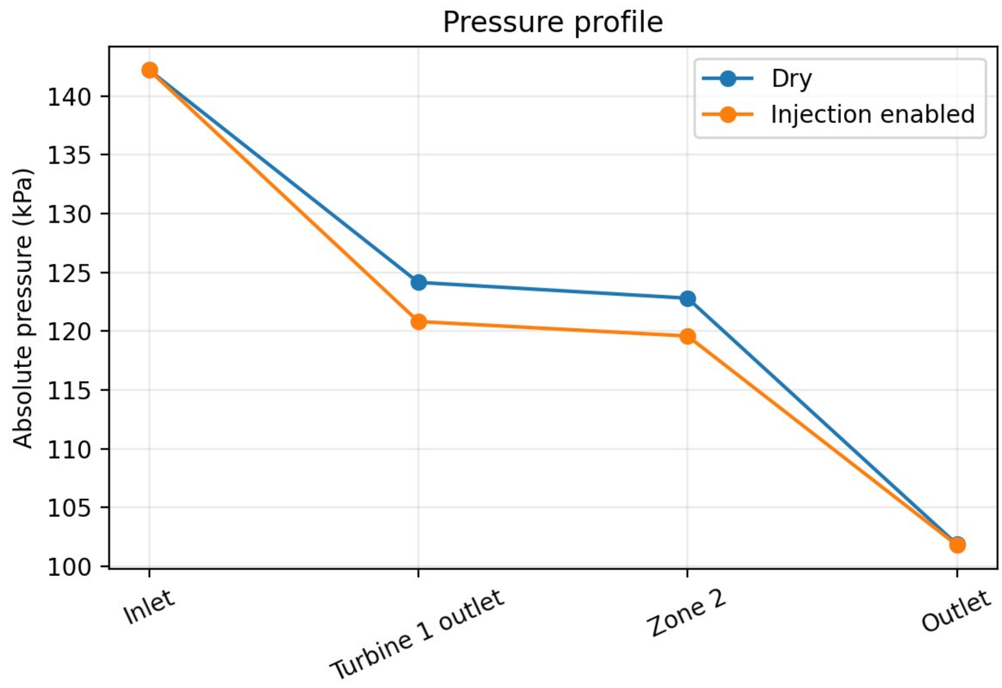

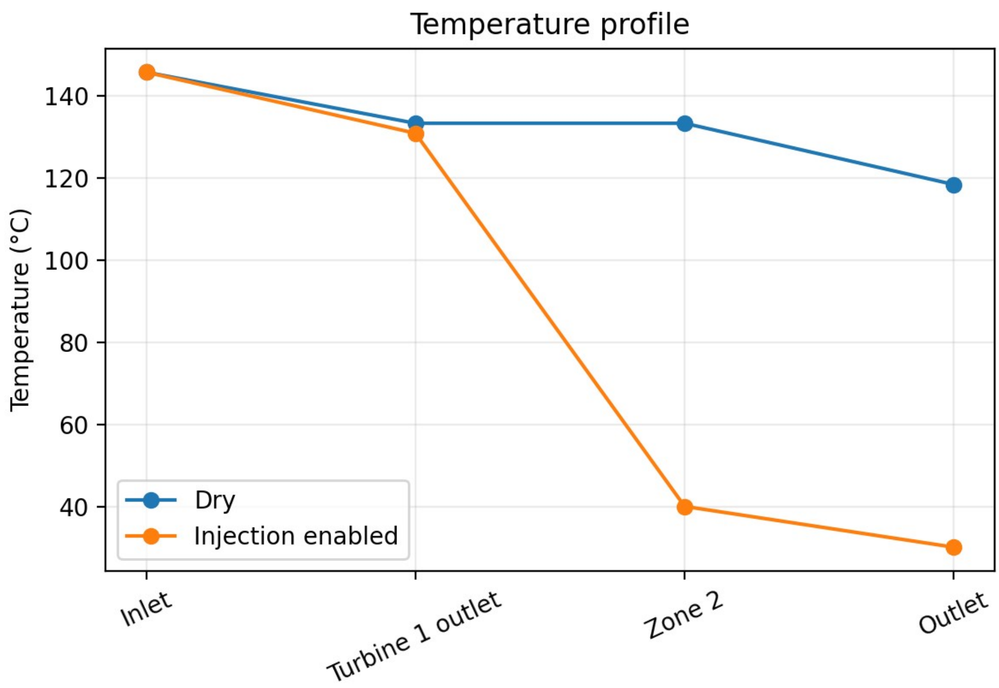

Figure 2. Pressure and temperature profiles at the best comparative point found.

One-factor effects

Input variable	Fine point of maximum Δ power	Maximum Δ power	Fine point of maximum paired gain	Maximum paired gain	Point of maximum injected power in fine window	Unit
Temperature	372.00	31.78	354.00	5.90	410.00	K
Pressure	168.00	29.72	107.00	5.74	190.00	kPa(a)
Velocity	34.00	24.63	34.00	5.00	28.00	m/s
Relative humidity	4.00	25.09	4.00	5.14	6.00	%

Each one-factor curve holds the other inlet variables at their nominal values. The peaks therefore show local trends for the tested configuration rather than universal optima.

Temperature: no injection benefit was selected at the cold end. The comparative benefit rose sharply once evaporation became effective, peaked in a moderate-to-hot interval, and then declined as constraints and outlet/leakage conditions dominated.

Pressure: absolute power generally increased with pressure until the tip-speed constraint ended the feasible fixed-design interval. Comparative percentage gain was largest near the low-pressure end because the dry baseline was smaller; incremental power peaked at an intermediate pressure.

Velocity: performance rose to a capacity-controlled region. Above the effective swallowing-capacity transition, additional available inlet velocity did not proportionally raise processed flow and could move the solution to a less favourable branch.

Humidity: low RH was strongly favourable. At nominal T, P and v, the optimiser selected zero injection at approximately 50% RH and above because the remaining evaporation benefit did not exceed its penalties.

Temperature and humidity determine how much evaporation is available, while pressure and velocity determine how much gas flow and turbine pressure drop the system can accept. The strongest benefit occurs in a limited combined operating region rather than at the maximum value of every input.

Figure 3 shows the effect of each inlet variable on the additional net power produced by injection.

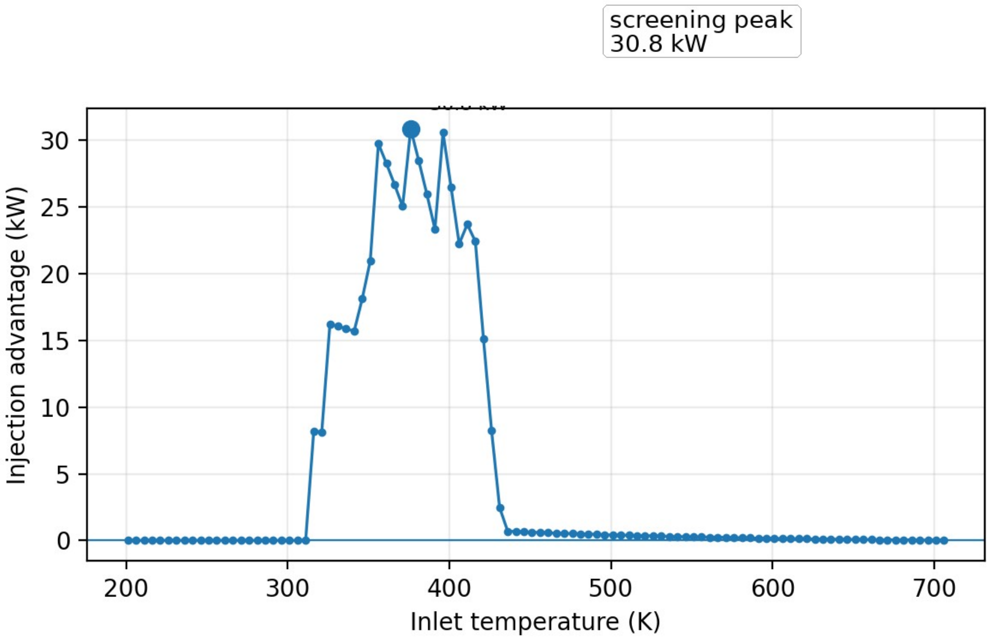
screening peak
30.8 kW
Injection advantage (kW)
0
5
10
15
20
25
30
200
300
400
500
600
700
Inlet temperature (K)

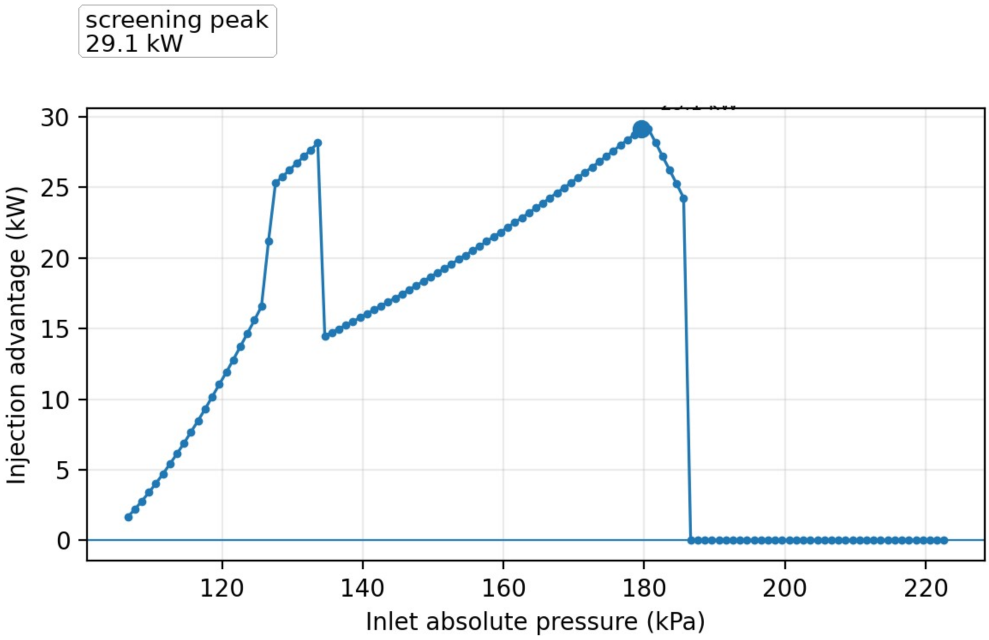
screening peak
29.1 kW
Injection advantage (kW)
0
5
10
15
20
25
30
120
140
160
180
200
220
Inlet absolute pressure (kPa)

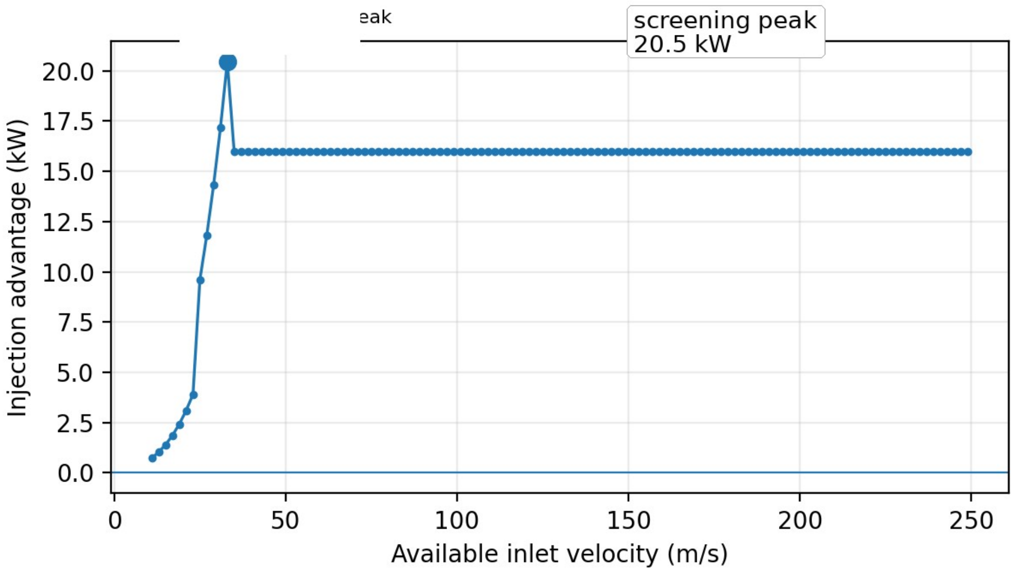

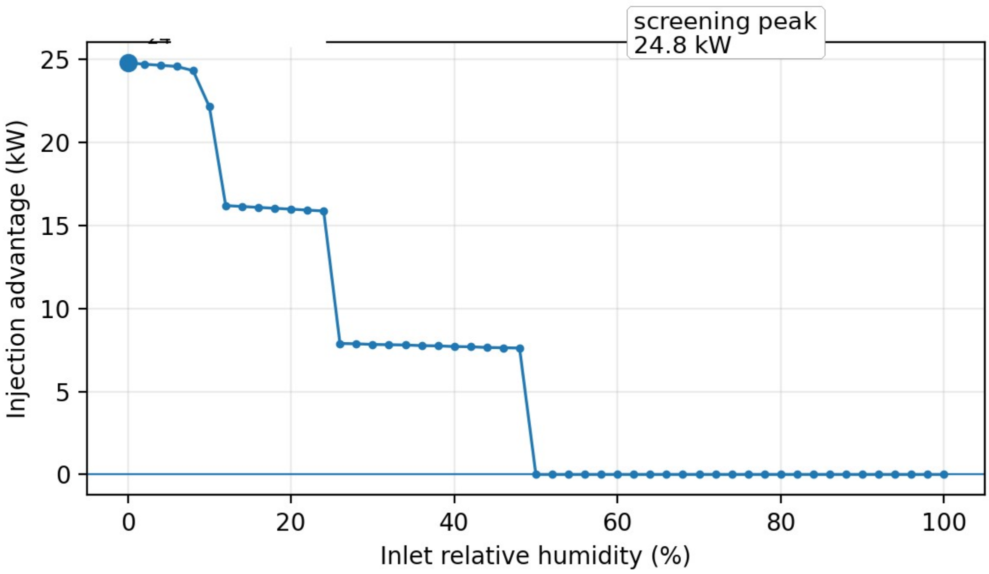

Figure 3. Effect of each inlet variable on the additional net power produced by injection.

Combined-parameter effects

Parameter pair	First coordinate at grid maximum	Second coordinate at grid maximum	Maximum Δ power	Paired gain
T × P	375.0 K	180.0 kPa(a)	41.39	1.38
T × v	395.8 K	37.5 m/s	37.15	5.85
T × RH	416.7 K	0.0 %	82.62	14.04
P × v	180.0 kPa(a)	37.5 m/s	35.47	1.31
P × RH	150.8 kPa(a)	8.3 %	38.18	2.51
v × RH	37.5 m/s	0.0 %	24.80	5.09

Figure 4 shows the combined effects of pairs of inlet variables. White areas were outside the feasible operating range.

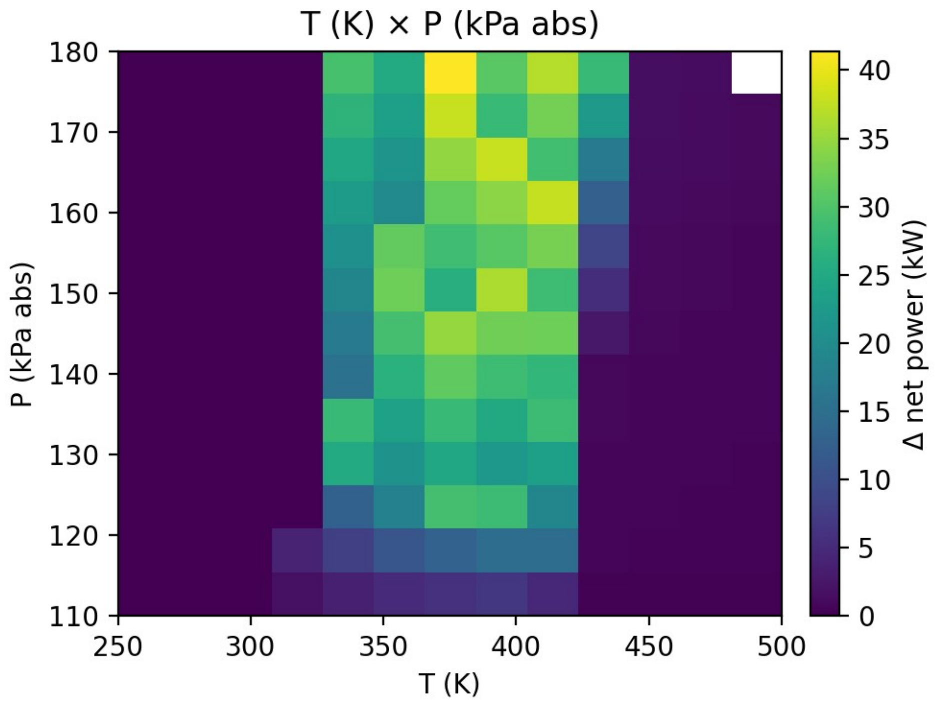
T (K) × P (kPa abs)
P (kPa abs)
180
170
160
150
140
130
120
110
250
300
350
400
450
500
T (K)
Δ net power (kW)
40
35
30
25
20
15
10
5
0

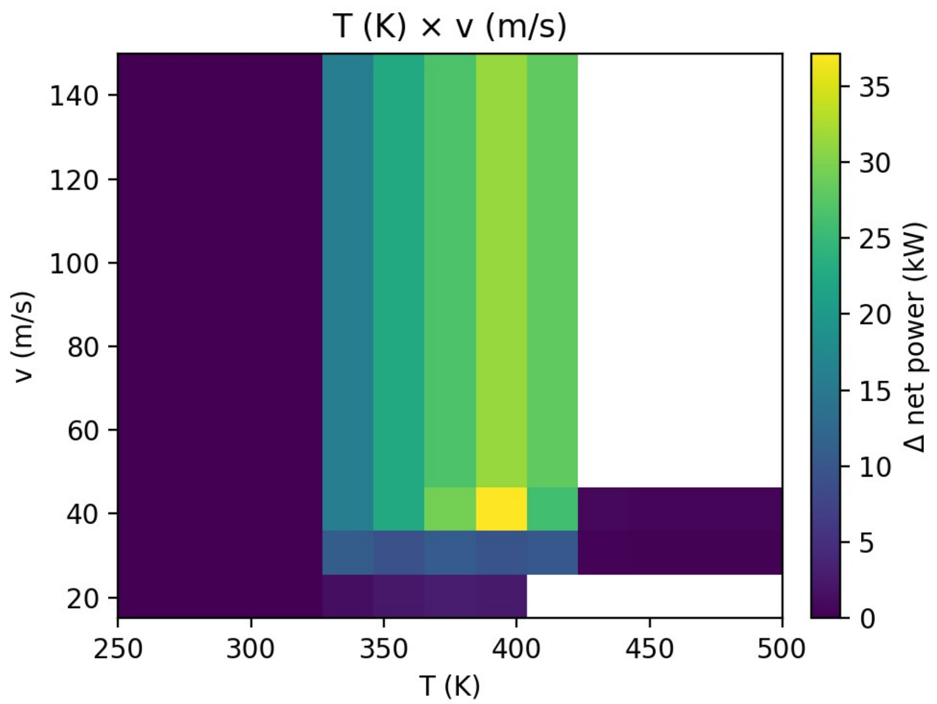
T (K) × v (m/s)
v (m/s)
140
120
100
80
60
40
20
250
300
350
400
450
500
T (K)
Δ net power (kW)
35
30
25
20
15
10
5
0

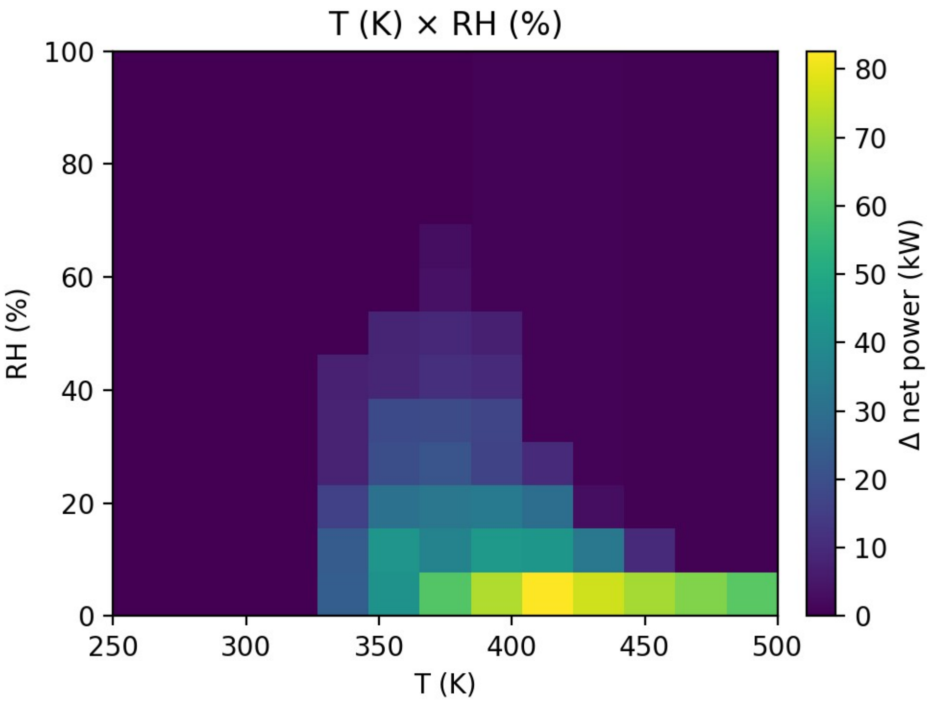
T (K) × RH (%)
RH (%)
100
80
60
40
20
0
250
300
350
400
450
500
T (K)
Δ net power (kW)
0
10
20
30
40
50
60
70
80

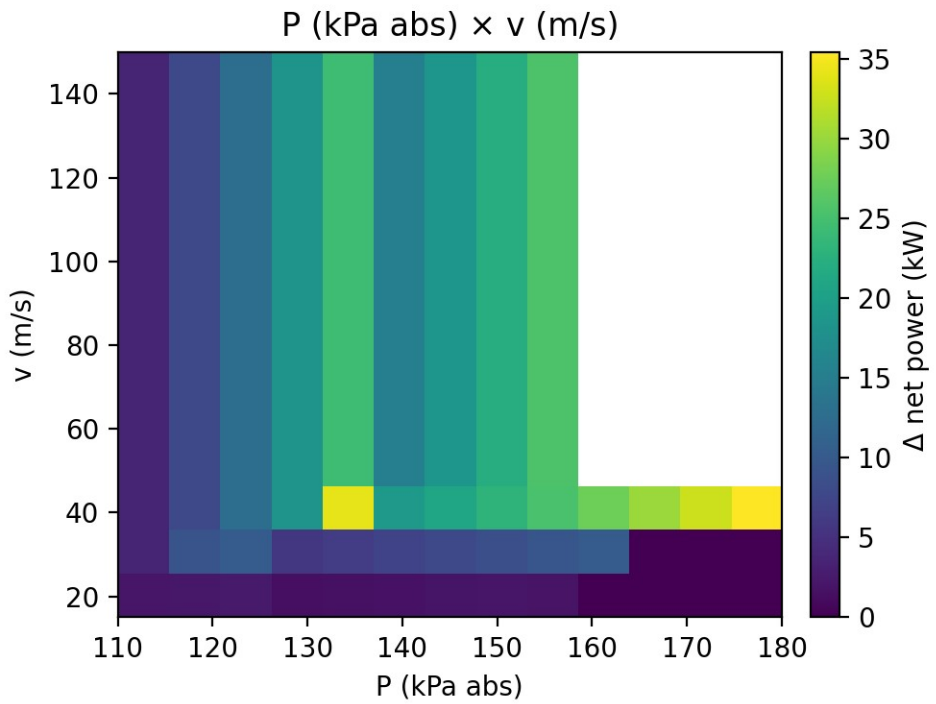
P (kPa abs) × v (m/s)
v (m/s)
140
120
100
80
60
40
20
110
120
130
140
150
160
170
180
P (kPa abs)
Δ net power (kW)
0
5
10
15
20
25
30
35

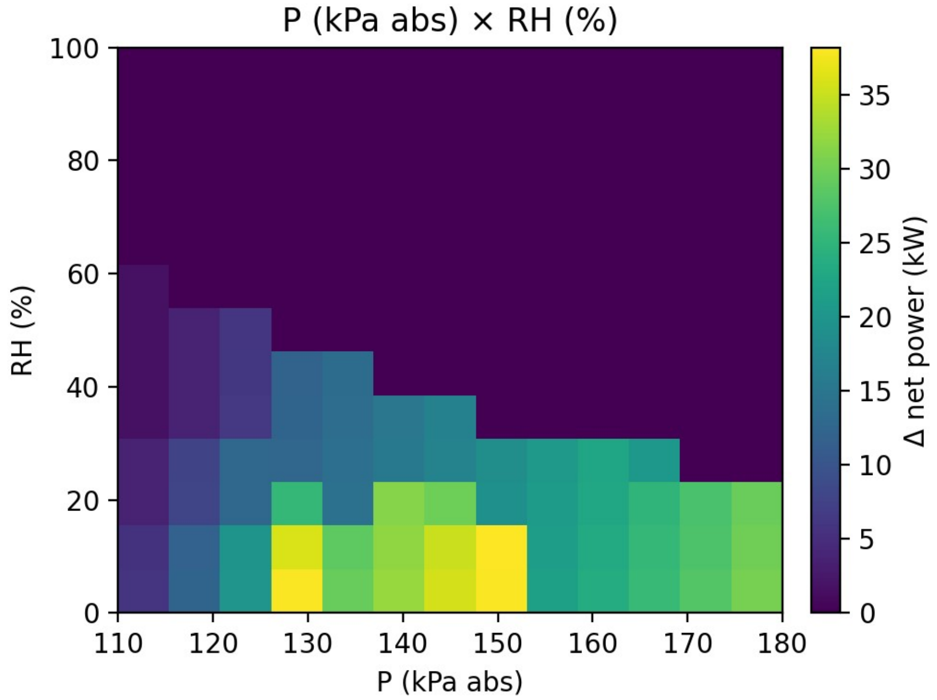

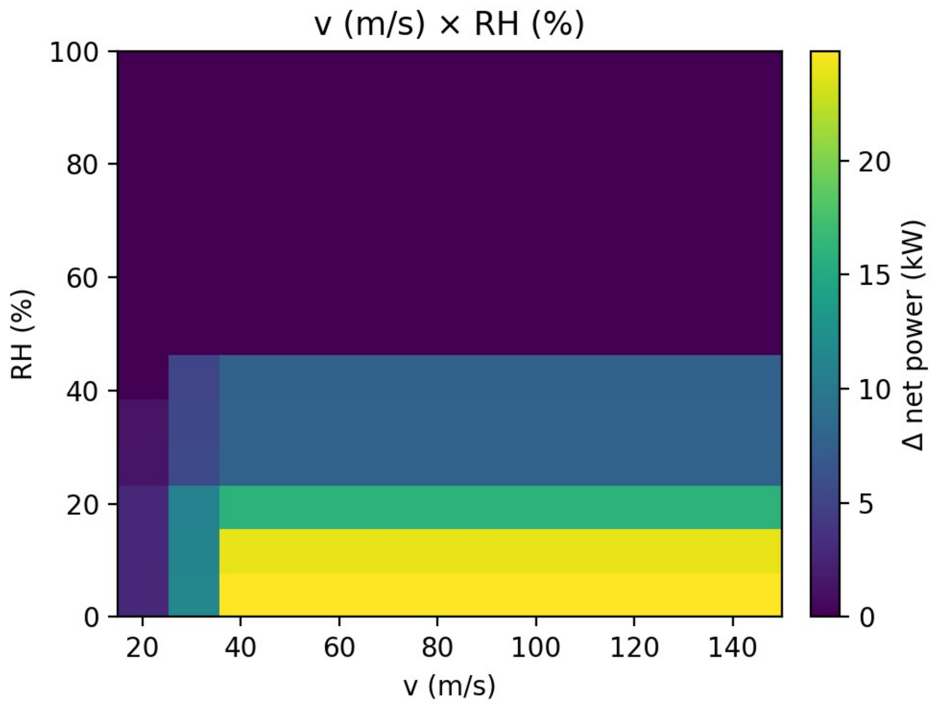

Figure 4. Combined effects of pairs of inlet variables. White areas were outside the feasible operating range.

Inlet conditioning and flow-management recommendations

Conditioning should be used only when it helps preserve the injection advantage, keeps the operating point inside the coupled pressure-flow constraints, or allows the stream to be shared safely among modules. It should not be applied automatically: cooling, throttling, dilution or dehumidification can reduce the pressure, temperature or mass-flow energy available to Turbine 1. The unconditioned dry and injection-enabled cases should therefore be calculated first, and a conditioning step should be accepted only when it increases net exported power or is required for safe operation.

Condition above favourable region	Recommended action
Temperature materially above about 419 K for the best comparative region	Blend with a cooler compatible stream or recover heat upstream while maintaining pressure and mass-flow accounting
Pressure above about 142 kPa(a) when maximising comparative gain	Use a pressure-recovery expander, staged inlet, bypass or pressure let-down before the tested module; do not describe pressure reduction as simple dilution
Velocity above the favourable module range near 45 m/s	Split flow across parallel modules, enlarge effective inlet area or bypass excess flow rather than throttle it
Humidity above the low-RH favourable range	Dehumidify or blend with dry gas; calculate on humidity ratio, not RH directly

The recommendations above are intended to preserve useful energy. Blending should use a compatible stream and retain complete mass and enthalpy accounting. Where pressure must be reduced, a pressure-recovery expander or staged process is preferable to a purely dissipative restriction. Excess velocity should be managed by parallel modules, increased effective area or bypass rather than indiscriminate throttling. Humidity control should be based on humidity ratio and dew-point behaviour because relative humidity changes with temperature and pressure.

Recommended control approach:

Control the system for maximum measured net exported power rather than for a fixed temperature or injection rate. The controller should compare the injection-enabled result with the dry baseline, reduce injection as the benefit narrows, and stop injection whenever the pump and auxiliary penalties exceed the additional Turbine 1 output. Pressure reserve, carryover, rotor-speed and flow constraints remain hard limits.

Conclusions

Best modelled point:

The strongest paired result within the tested search space occurred at T = 419 K, P = 142.2 kPa(a), v = 45 m/s and RH = 0%. The model predicted an increase of 220.5 kW, or 19.27%, over the dry case. This is the best point found by the stated search procedure and should not be interpreted as proof of a unique global optimum.

Geometry and active bounds:

The maximum-output design repeatedly moved to the declared upper limits for common flow area and Zone 2 length and to the minimum droplet-size limit: $A_1 = A_2 = 2\ m^2$, L = 8 m and $D_{32} = 20\ \mu m$. These active bounds show that the present optimum is constrained by the search domain; larger area, greater residence length or a different atomiser range would require separate testing.

Injection-rate boundary:

The optimum liquid-to-dry-gas ratio was close to the configured upper bound of 0.04 kg/kg. A higher ratio might change the optimum, but that range was not tested because this report preserves the simulator default. No benefit above the tested bound should therefore be assumed.

Favourable inlet conditions:

Very dry gas and moderate-to-high inlet temperature were the strongest promoters of comparative benefit. As humidity increased, the available evaporation effect and incremental benefit declined; at sufficiently high humidity, zero injection became the optimal modelled operating choice.

Absolute and comparative objectives:

Higher inlet pressure can increase absolute electrical output while reducing the percentage advantage of injection because the dry baseline also becomes stronger. Absolute injection-enabled output, incremental power and percentage gain should therefore be reported separately.

Design and control interpretation:

The tested response contains branch changes and hard-constraint boundaries. A practical design should use bounded operating windows and a controller that continuously checks net-power improvement, rather than relying on one exact target point.

APPENDIX C1

SIMULATOR INTERFACE AND REPRODUCIBLE DEMONSTRATION RUN

C1.1 Purpose and engineering use

This appendix presents the principal user-interface pages of the System Performance and Design Optimisation Simulator supplied as part of the patent and technology package. The image sheets document the engineering inputs used for the best-found comparative operating point, the resulting dry and injection-enabled performance calculation, and the mathematical-model documentation embedded within the simulator.

The simulator is intended to assist engineers in evaluating a known gas-flow source. The engineer enters the available inlet temperature, absolute pressure, gas-flow velocity, relative humidity, ambient conditions and intended operating duration, together with applicable design limits and component assumptions. The simulator then evaluates feasible system dimensions, liquid-injection requirements, evaporation performance, pressure and temperature behaviour, auxiliary demands and comparative net electrical output.

The simulator compares the injection-enabled arrangement with the same physical configuration operating without liquid injection. Its purpose is to support engineering screening, comparative design development and identification of favourable operating settings for known input conditions. It does not replace detailed mechanical design, calibrated component maps, computational fluid-dynamics analysis, safety assessment and commissioning.

C1.2 Demonstration operating conditions

The demonstration run demonstrates the best-found comparative operating point reported in Annexure C. The specified inlet conditions are 419 K (145.9°C), 142.2 kPa absolute pressure, an available gas-flow velocity of 45.0 m/s and 0% inlet relative humidity. The ambient conditions are 101.325 kPa absolute pressure, 298.15 K and 50% relative humidity, and the operating duration is eight hours.

C1.3 Results

The simulator selected a common flow area of 2.00 m², a cooling and evaporation length of 8.00 m, a target droplet diameter of 20 µm and a liquid-to-dry-gas mass ratio of 0.03926 kg/kg. These values correspond to the best-found design reported in the principal comparative analysis.

The calculation returned the following results:

> Dry net electrical power: 1.144085 MW
>
> Injection-enabled net electrical power: 1.364583 MW
>
> Additional net electrical output: 220.498 kW
>
> Modelled paired increase: 19.2728%
>
> Additional net energy over eight hours: approximately 1.764 MWh

ANNEXURE C

US Patent 12,650,086 B1: Device for Conversion of Kinetic and Thermal Energies of Gas Flows to Work

Comparative-Energy Report

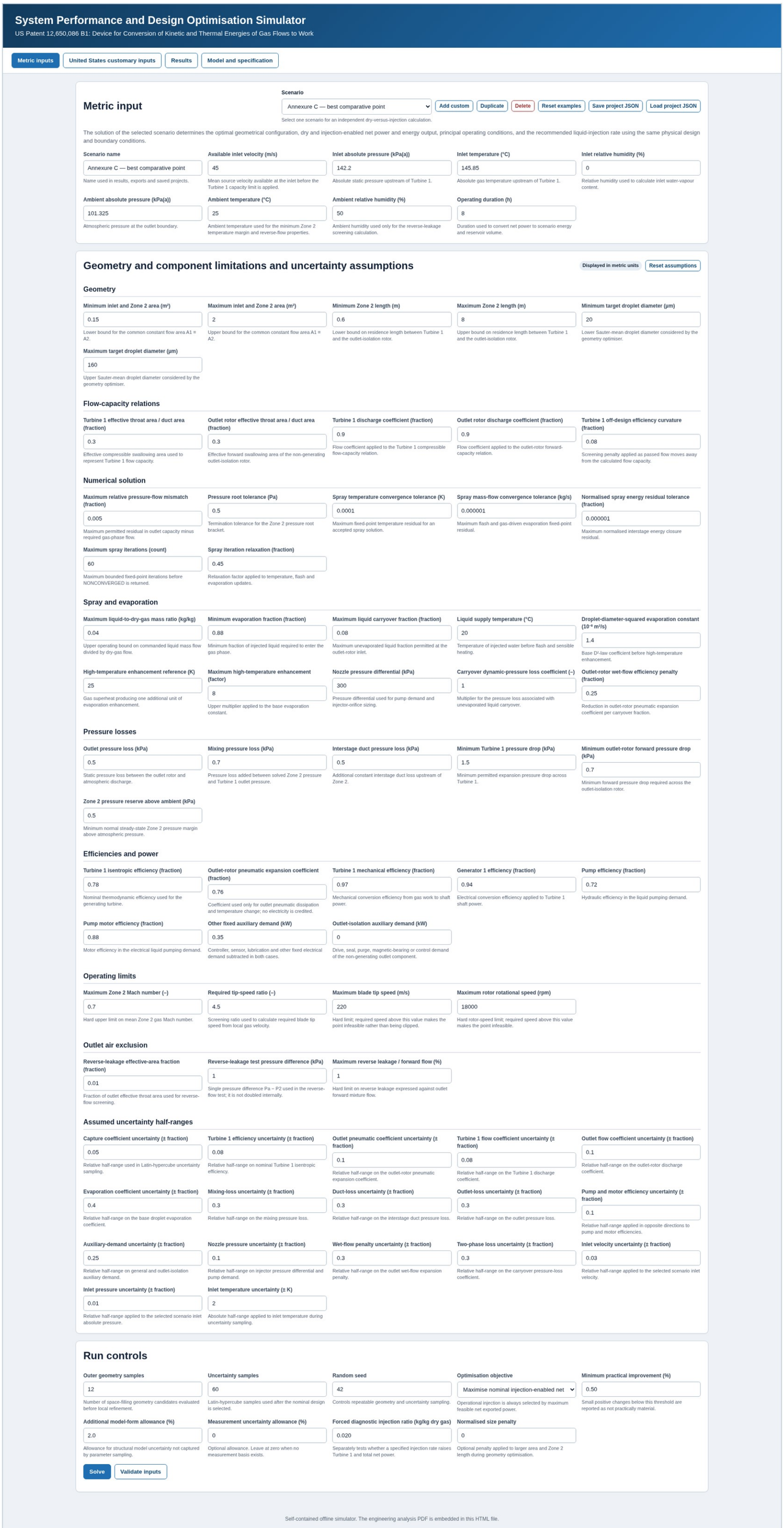

Figure C1. Simulator input interface demonstrating the best-found comparative operating conditions. The page records the known gas-stream and ambient conditions, operating duration, design limits, component assumptions, uncertainty allowances and optimisation objective used for the calculation.

System Performance and Design Optimisation Simulator

US Patent 12,650,086 B1: Device for Conversion of Kinetic and Thermal Energies of Gas Flows to Work

Metric inputs | United States customary inputs | Results | Model and specification

Results

Download conclusion TXT | Download log TXT | Download results CSV | Download results JSON | Download figures SVG

Recommended geometrical configuration

Calculated parameter	Value	Unit
Constant area A1 = A2	2	m²
Equivalent duct diameter	1.5958	m
Zone 2 length	8	m
Target droplet diameter	20	µm
Required Turbine 1 tip speed	194.4	m/s
Required outlet-rotor tip speed	183.78	m/s
Required rotor speeds	2,078 / 1,964	rpm
Nozzle count	453	count
Liquid reservoir	144.66	m³

Dry baseline and optimised injection

Quantity	Dry baseline	Optimised injection	Difference or note
Liquid-to-dry-gas ratio	0	0.03926	0.03926
Liquid flow	0 kg/s	4.01025 kg/s	4.01025 kg/s
Zone 2 pressure	122.8068 kPa(a)	119.5889 kPa(a)	-3.2179 kPa(a)
Zone 2 temperature	133.418 °C	40.195 °C	-93.223 °C
Gas-phase outlet flow	102.14795 kg/s	106.1582 kg/s	4.01025 kg/s
Turbine 1 electrical output	1,144.4351 kW	1,366.9514 kW	222.5162 kW
Pump demand	0 kW	2.0184 kW	2.0184 kW
Outlet pneumatic dissipation	1,489.5646 kW	1,068.4096 kW	-421.155 kW
Outlet electrical credit	0 W	0 W	0 W
Net exported power	**1,144.0851 kW**	**1,364.5829 kW**	**19.2728%**
Scenario net energy	9,152.6812 kWh	10,916.6634 kWh	1,763.9823 kWh
Evaporation fraction	—	100%	high-temperature evaporation
Flash / gas-driven evaporation	—	0 / 4.010252 kg/s	liquid availability
Forced diagnostic net-power change	—	0.02 kg/kg	10.2747%

Numerical closure and model diagnostics

Diagnostic	Dry baseline	Optimised injection
Structured status	CONVERGED_FEASIBLE	CONVERGED_FEASIBLE
Zone 2 pressure iterations	18	14
Spray iterations	0	26
Forward-flow mismatch	0.000059%	0.000282%
Normalised total-mass residual	0.000e+0	0.000e+0
Normalised water-species residual	0.000e+0	0.000e+0
Normalised spray-energy residual	0.000e+0	1.659e-7
Net-power accounting residual	0.000e+0 W	0.000e+0 W
Property-domain status	VALID	VALID
Local saturation temperature	105.452 °C	104.685 °C
Local latent heat	2,239.824 kJ/kg	2,242.255 kJ/kg
Gas / liquid superheat	27.966 / -85.452 K	26.308 / -84.685 K
Effective evaporation coefficient	2.966e-8	2.873e-8
Reverse leakage / forward flow	0.2551%	0.2455%
Active evaporation regime	no injection	high-temperature evaporation

Dry and injection net power

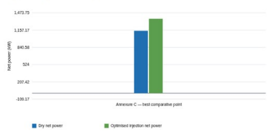

Injection sweep

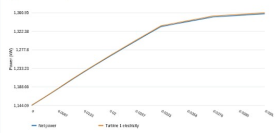

Injection effect on pressure

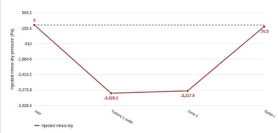

Temperature profile

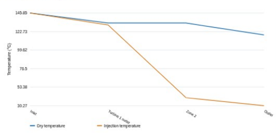

Run log

```
2026-07-12T01:19:20.365Z  RUN START; scenario=Annexure C — best comparative point; Section 17 outlet-isolation constant-area case; geometry samples=12; uncertainty samples=60;
objective=injection-power.
2026-07-12T01:19:20.365Z  Materiality threshold=max(practical 0.5%, model-form 2%, measurement 0%)=2%.
2026-07-12T01:19:25.206Z  Nominal dry net power=1144085.14381 W; injection net power=1364582.93027 W; paired change=19.27285%.
2026-07-12T01:19:25.206Z  Uncertainty: feasible=45/60; P05=11.25797%; median=15.72021%; P95=21.29211%; probability above threshold=100%.
2026-07-12T01:19:25.206Z  Static verification: 9/9 required tests passed.
2026-07-12T01:19:25.206Z  CONCLUSION ROBUST_MODELLED_ADVANTAGE: The declared model predicts a robust net-power advantage.
```

Self-contained offline simulator. The engineering analysis PDF is embedded in this HTML file.

Figure C2. Simulator results for the best-found comparative operating conditions. The page records the recommended system configuration, dry and injection-enabled net electrical output, selected liquid-injection rate, comparative gain, pressure and temperature response, auxiliary demands, numerical diagnostics and active engineering constraints.

System Performance and Design Optimisation Simulator

US Patent 12,650,086 B1: Device for Conversion of Kinetic and Thermal Energies of Gas Flows to Work

Metric inputs | United States customary inputs | Results | Model and specification

Model description

The accompanying engineering document develops a mathematical framework for the two-stage gas-flow energy-conversion device described in US Patent 12,650,086 B1. The broader framework covers turbine performance, conventional spray evaporation, pressure-dependent saturation, flash evaporation, high-temperature gas-driven evaporation, coupled mass, water-species and energy balances, pressure losses, net power, system sizing, constraints, optimisation, control and verification.

Specific operable case considered

The inlet and Zone 2 areas are equal; the downstream rotor receives no electrical-generation credit; Zone 2 pressure is solved from the forward-flow compatibility of Turbine 1, the evaporating interstage control volume and the outlet-isolation rotor; outlet-isolation auxiliary demand is subtracted; and the dry baseline uses the same physical design and boundary conditions with liquid injection set to zero.

Comprehensive mathematical model

The patented system consists of a first turbine, an interstage liquid-injection and evaporative-cooling zone, a second turbine near the atmospheric outlet, pressure and temperature sensing, and a controller regulating the injection rate. The model below converts that architecture into a constrained dynamic optimisation problem.[8]

Atmospheric pressure and temperature are fixed:

(23) $P_a = P_a, T_a = T_a$

All other operating, control and design quantities may vary.

1. System stations

Define four principal stations:

(24) 1 : Zone 1, upstream of turbine 1

(25) $1e$: outlet of turbine 1, before liquid injection

(26) 2 : Zone 2, after evaporation and before turbine 2

(27) 3 : outlet of turbine 2, upstream of the outlet duct, screen, diffuser and final atmospheric-discharge losses

The required nominal pressure and temperature hierarchy is:

(28) $P_1 > P_2 > P_a$

(29) $T_1 > T_2 > T_a$

The outlet station normally satisfies:

(30) $P_3 = P_a + \Delta P_{exit} \geq P_a$

At the final atmospheric-discharge plane, the static pressure is P_a. The final atmospheric plane is a boundary condition and is not included as a dynamic state.

2. Variable classification

2.1 State vector

A suitable lumped dynamic state vector is

(31) $$x(t) = \begin{bmatrix} P_1 & T_1 & P_{1e} & T_{1e} & P_2 & T_2 & P_3 & T_3 \\ M_1 & M_2 & M_{v,2} & M_{l,2} & \Omega_1 & \Omega_2 & T_{w,1} & T_{w,2} \end{bmatrix}^T$$

where:

- M_k is the gas or gas–vapour mass stored in zone k;
- $M_{v,2}$ is the vapour mass in Zone 2;
- $M_{l,2}$ is the suspended unevaporated liquid mass;
- Ω_j is turbine angular velocity of turbine j;
- $T_{w,k}$ is a representative duct-wall temperature.

2.2 Control vector

(32) $$u(t) = [\dot{m}_l \quad P_{inj} \quad \tau_{g,1} \quad \tau_{g,2} \quad x_v \quad \beta_1 \quad \beta_2]^T$$

[8] de St. Amatus, B. and de St. Amatus, A. (2026) *Device for conversion of kinetic and thermal energies of gas flows to work*. US Patent 12,650,086 B1, 9 June.

23

Figure C3. Mathematical model and engineering specification embedded within the simulator. The page summarises the simulator's thermodynamic, flow, evaporation, power, optimisation, control and verification framework.